PHYSICAL REVIEW D **75,** 094008 (2007)

Generalized z-scaling in proton-proton collisions at high energies

I. Zborovský*
Nuclear Physics Institute, Academy of Sciences of the Czech Republic, Řež, Czech Republic

M. V. Tokarev†
Joint Institute for Nuclear Research, Dubna, Russia
(Received 19 June 2006; published 8 May 2007)

New generalization of the z-scaling in inclusive particle production is proposed. The scaling variable z is a fractal measure which depends on kinematic characteristics of the underlying subprocess expressed in terms of the momentum fractions x_1 and x_2 of the incoming protons. In the generalized approach, x_1 and x_2 are functions of the momentum fractions y_a and y_b of the scattered and recoil constituents carried by the inclusive particle and recoil object, respectively. The scaling function $\psi(z)$ for charged and identified hadrons produced in proton-proton collisions is constructed. The fractal dimensions and heat capacity of the produced medium entering definition of the variable z are established to restore energy, angular, and multiplicity independence of $\psi(z)$. The proposed scheme allows a unique description of data on inclusive cross sections at high energies. Universality of the shape of the scaling function for various types of produced hadrons (π, K, $\bar{p}$, Λ) is shown. Results of the analysis of experimental data are compared with the next-to-leading order (NLO) QCD calculations in p_T and z-presentations. The obtained results suggest that the z-scaling may be used as a tool for searching for new physics phenomena of particle production in high transverse momentum and the high multiplicity region at proton-proton colliders RHIC and LHC.

DOI: 10.1103/PhysRevD.75.094008 PACS numbers: 13.85.Ni, 13.85.−t, 13.87.Fh

I. INTRODUCTION

The production of particles with high transverse momenta from the collision of hadrons and nuclei at sufficiently high energies has relevance to constituent interactions at small scales. In this regime, it is interesting to search for new physical phenomena in elementary processes such as quark compositeness [1], extra dimensions [2], black holes [3], fractal space-time [4], etc. Other aspects of high energy interactions are connected with small momenta of secondary particles and high multiplicities. This regime has relevance to collective phenomena of particle production. The search for new physics in both regions is one of the main goals of investigations at Relativistic Heavy Ion Collider (RHIC) at BNL and Large Hadron Collider (LHC) at CERN. Experimental data on particle production can provide constraints for different theoretical models. Processes with high transverse momenta of produced particles are most suitable for a precise test of perturbative quantum chromodynamics (QCD). The soft regime is suitable for the verification of nonperturbative QCD and investigation of phase transitions in non-Abelian theories.

Nucleus-nucleus interactions are very complicated. In order to understand their nature one often exploits phenomenology and comparison with simpler proton-proton and proton-nucleus collisions. Many approaches to the description of particle production are used to search for regularities reflecting general principles in these systems at high energies [5–14]. One of the most basic principles is the self-similarity of hadron production valid both in soft and hard physics. Other general principles are locality and fractality which can be applied to hard processes at small scales. The locality of hadronic interactions is confirmed by results from numerous experimental and theoretical studies. These investigations have shown that the interactions of hadrons and nuclei can be described in terms of the interactions of their constituents. Fractality in hard processes is a specific feature connected with the substructure of the constituents. This includes the self-similarity over a wide scale range.

Fractality of soft processes concerning the multiparticle production was investigated by many authors [15–17]. Fractality in inclusive reactions with high-p_T particles was considered for the first time in the framework of the z-scaling [18]. The approach is based on principles of locality, self-similarity, and fractality. It takes into account the fractal structure of the colliding objects, the interaction of their constituents, and particle formation. The scaling function $\psi(z)$ and the variable z are constructed using the experimentally measured inclusive cross section $Ed^3\sigma/dp^3$ and the multiplicity density $dN/d\eta$. In the original version [18], the construction was based on the assumption that gross features of the inclusive particle distribution for the inclusive reaction

$$M_1 + M_2 \rightarrow m_1 + X \tag{1}$$

at high energies can be described in terms of the corresponding exclusive subprocess

$$(x_1M_1) + (x_2M_2) \rightarrow m_1 + (x_1M_1 + x_2M_2 + m_2). \tag{2}$$

*Electronic address: zborovsky@ujf.cas.cz
†Electronic address: tokarev@sunhe.jinr.ru

Here M_1 and M_2 are the masses of the colliding hadrons (or nuclei) and m_1 is the mass of the inclusive particle. The mass parameter m_2 is introduced in connection with internal conservation laws (for isospin, baryon number, strangeness, ...). The symbols x_1 and x_2 stand for momentum fractions of the incoming four-momenta P_1 and P_2 of the colliding objects. The scaling variable z was constructed as a fractal measure with a characteristic power dependence on the nucleon fractal dimension δ in space of the momentum fractions $\{x_1, x_2\}$. The scale of the variable z was determined to be proportional to the dynamical quantity-average multiplicity density $dN_{ch}/d\eta|_0$ of charged particles produced in the central region of the interaction ($\eta = 0$). The z-scaling for nonbiased collisions was established as the independence of the scaling function $\psi(z)$ on the collision energy $\sqrt{s}$ and the angle θ of the inclusive particle for a single constant value of δ.

The concept of the z-scaling was generalized for various multiplicities N_{ch} of produced particles [19]. The relation of the z-scaling to the entropy S and the heat capacity c of the colliding system was found. The generalization was connected with the introduction of a momentum fraction y in the final state written in the symbolic form

$$(x_1M_1) + (x_2M_2) \rightarrow (m_1/y) + (x_1M_1 + x_2M_2 + m_2/y). \tag{3}$$

It was shown that the generalized scaling represents a regularity in both the soft and hard regime in proton-(anti)proton collisions over a wide range of initial energies and multiplicities of the produced particles. However, the generalization of the scaling for various multiplicities was obtained at the expense of the angular independence of the scaling function observed for $y = 1$ [18].

In this paper we show that independence of the scaling function $\psi(z)$ on the collision energy $\sqrt{s}$, multiplicity density $dN_{ch}/d\eta$, and the production angle θ can be restored simultaneously, if two fractions y_a and y_b for the scattered constituent and its recoil are introduced, respectively. The paper is organized as follows. A concept of the generalized z-scaling and the method of construction of the scaling function $\psi(z)$ are described in Sec. II. Results of the analysis of experimental data on inclusive cross sections of hadrons produced in pp collisions in the z-presentation are given in Sec. III. We have analyzed the transverse momentum spectra of the charged particles, negative pions, kaons, antiprotons, and Λ's measured at ISR and RHIC energies. Calculations of hadron spectra in the next-to-leading order of QCD are presented in Sec. IV. Predictions based on the CTEQ5m parton densities and KKP fragmentation functions are confronted with the scaling function $\psi(z)$ in the region of large z. The discussion of the possible parallels with the pQCD is presented in Sec. V. Conclusions are summarized in Sec. VI. Some ideas concerning physical interpretation of the variable z are mentioned in Appendix A. Appendix B contains formulae for the transformation from the variables p_T and y to the variables z and η used in the z-presentation of the experimental cross sections.

II. NEW GENERALIZATION OF THE z-SCALING

The collision of extended objects like hadrons and nuclei at sufficiently high energies is considered as an ensemble of individual interactions of their constituents. The constituents are partons in the parton model or quarks and gluons in the theory of QCD. A single interaction of constituents is illustrated in Fig. 1. Structures of the colliding objects are characterized by parameters δ_1 and δ_2. Interacting constituents carry the fractions x_1 and x_2 of the momenta P_1 and P_2 of the incoming objects. The inclusive particle carries the momentum fraction y_a of the scattered constituent with a fragmentation characterized by a parameter ϵ_a. A fragmentation of the recoil constituent is described by ϵ_b and the momentum fraction y_b. Multiple interactions are considered to be similar. This property represents a self-similarity of the hadronic interactions at the constituent level.

A. Momentum fractions x_1, x_2, y_a, and y_b

The idea of the z-scaling is based on the assumption [10] that gross features of an inclusive particle distribution of the reaction (1) can be described at high energies in terms of the kinematic characteristics of the corresponding constituent subprocesses. We consider the subprocess to be a binary collision

$$(x_1M_1) + (x_2M_2) \rightarrow (m_1/y_a) + (x_1M_1 + x_2M_2 + m_2/y_b) \tag{4}$$

of the constituents (x_1M_1) and (x_2M_2) resulting in the

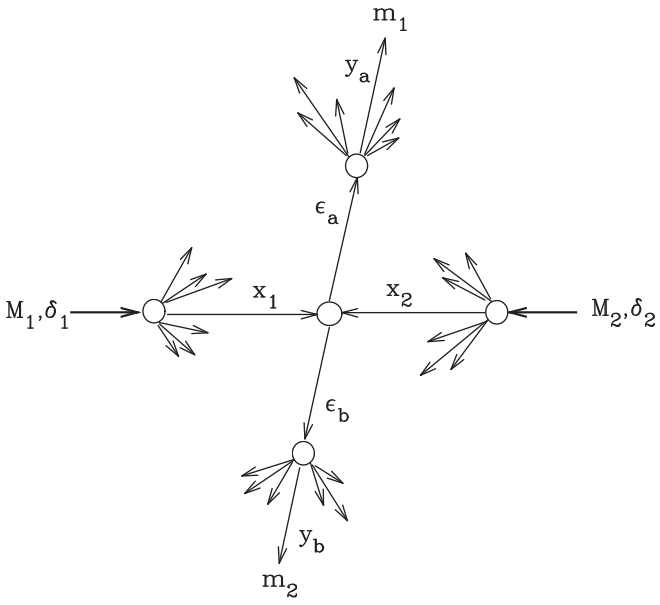

FIG. 1. Diagram of the constituent subprocess.

scattered (m_1/y_a) and recoil $(x_1M_1 + x_2M_2 + m_2/y_b)$ objects in the final state. The inclusive particle with the mass m_1 and the 4-momentum p carries the fraction y_a of the 4-momentum of the scattered constituent. Its counterpart (m_2), moving in the opposite direction, carries the 4-momentum fraction y_b of the produced recoil. The binary subprocess is subject to the condition

$$(x_1P_1 + x_2P_2 - p/y_a)^2 = (x_1M_1 + x_2M_2 + m_2/y_b)^2. \tag{5}$$

The associate production of (m_2) ensures conservation of the quantum numbers. Besides the main channel the parameter m_2 makes it possible to take into account contributions from additional channels with the production of any particles or states.

Let us take for definiteness inclusive production of K^- mesons in proton-proton collisions. The main channel of K^- production is usually considered with the simultaneous formation of the K^+ meson. The corresponding value of the parameter m_2 is determined by means of the exclusive reaction $p + p \to K^- + p + p + K^+$. Using Eq. (5) for $x_1 = x_2 = y_a = y_b = 1$, we get $m_2 = m(K^+)$ in this case. Strangeness conservation allows also other reaction channels than the main whose effect, in specific kinematics, must not be negligible compared with the dominant channel. Possible configurations including production of the associate particles such as $\bar{\Lambda}$ or $\bar{\Sigma}$ can be effectively taken into account by using somewhat larger values of m_2. In the next section we will demonstrate that the main channel dominance with respect to the determination of m_2 is a reasonable assumption for the kinematical range of data analyzed in this paper.

Equation (5) is an expression of the locality of the hadron interaction at a constituent level. It represents a kinematic constraint on the momentum fractions x_1, x_2, y_a, and y_b which determine a subprocess (4). Next we introduce the function

$$\Omega(x_1, x_2, y_a, y_b) = (1 - x_1)^{\delta_1}(1 - x_2)^{\delta_2}(1 - y_a)^{\epsilon_a}(1 - y_b)^{\epsilon_b} \tag{6}$$

which connects the momentum fractions with structural characteristics δ_1, δ_2, ϵ_a, and ϵ_b of the interacting objects. Physical interpretation of Ω is given in Appendix A. For proton-proton collisions we set $\delta_1 = \delta_2 \equiv \delta$. In the case of nucleus-nucleus collisions $\delta_1 = A_1\delta$ and $\delta_2 = A_2\delta$, where A_1, A_2 are atomic numbers [18]. We assume that the fragmentation of the scattered and recoil constituents can be described by the same parameter $\epsilon \equiv \epsilon_a = \epsilon_b$ which depends on the type of the inclusive particle. For given values of δ and ϵ, we determine the fractions x_1, x_2, y_a, and y_b in a way to maximize the function $\Omega(x_1, x_2, y_a, y_b)$, simultaneously fulfilling condition (5). The momentum fractions x_1 and x_2 obtained in this way can be decomposed as follows

$$x_1 = \lambda_1 + \chi_1, \qquad x_2 = \lambda_2 + \chi_2. \tag{7}$$

Using the decomposition, the subprocess (4) can be rewritten in a symbolic form

$$x_1 + x_2 \to (\lambda_1 + \lambda_2) + (\chi_1 + \chi_2). \tag{8}$$

This relation means that the λ-parts of the interacting constituents contribute to the production of the inclusive particle, while the χ-parts are responsible for the creation of its recoil. The $\lambda's$ are functions of y_a and y_b (see Appendix A),

$$\lambda_1 = \kappa_1/y_a + \nu_1/y_b, \qquad \lambda_2 = \kappa_2/y_a + \nu_2/y_b, \qquad \lambda_0 = \bar{\nu}_0/y_b^2 - \nu_0/y_a^2, \tag{9}$$

where

$$\kappa_1 = \frac{(P_2p)}{(P_1P_2) - M_1M_2}, \qquad \kappa_2 = \frac{(P_1p)}{(P_1P_2) - M_1M_2}, \tag{10}$$

$$\nu_1 = \frac{M_2m_2}{(P_1P_2) - M_1M_2}, \qquad \nu_2 = \frac{M_1m_2}{(P_1P_2) - M_1M_2}, \tag{11}$$

$$\nu_0 = \frac{0.5m_1^2}{(P_1P_2) - M_1M_2}, \qquad \bar{\nu}_0 = \frac{0.5m_2^2}{(P_1P_2) - M_1M_2}. \tag{12}$$

The $\chi's$ are expressed via $\lambda's$ as follows

$$\chi_1 = \sqrt{\mu_1^2 + \omega_1^2} - \omega_1, \qquad \chi_2 = \sqrt{\mu_2^2 + \omega_2^2} + \omega_2, \tag{13}$$

where

$$\mu_1^2 = (\lambda_1\lambda_2 + \lambda_0)\alpha\frac{1 - \lambda_1}{1 - \lambda_2}, \qquad \mu_2^2 = (\lambda_1\lambda_2 + \lambda_0)\alpha^{-1}\frac{1 - \lambda_2}{1 - \lambda_1}, \tag{14}$$

and $\omega_i = \mu_i U$ $(i = 1, 2)$. The quantity

$$U = \frac{\alpha - 1}{2\sqrt{\alpha}}\,\xi \tag{15}$$

is proportional to the kinematical factor

$$\xi = \sqrt{\frac{\lambda_1\lambda_2 + \lambda_0}{(1 - \lambda_1)(1 - \lambda_2)}}, \tag{16}$$

$(0 \le \xi \le 1)$ and depends on the ratio of $\alpha = \delta_2/\delta_1$. It vanishes for collisions of the identical objects $(\delta_1 = \delta_2)$. The maximum of the function (6) with the condition (5) can be obtained by searching for the unconstrained maximum of the function

$$F(y_a, y_b) \equiv \Omega(x_1(y_a, y_b), x_2(y_a, y_b), y_a, y_b) \tag{17}$$

of two independent variables y_a and y_b. Here $x_i(y_a, y_b)$ are given explicitly by the expressions (7) and (9)–(16). There exists a single maximum of the function $F(y_a, y_b)$ for every value of the momentum p in the allowable kinematic region. Values of y_a and y_b corresponding to this maximum have been determined numerically. Having obtained x_1, x_2, y_a, and y_b, we evaluate the function Ω according to Eq. (6). For fixed numbers δ and ϵ we obtain in this way the maximal value of Ω for every momentum p of the inclusive particle.

Since the momentum fractions are determined by means of the maximization of the expression (6), they implicitly depend on δ and ϵ. The parameter ϵ enables to take effectively into account also prompt resonances out of which the inclusive particle of a given type may be created. Without changing the mass parameter m_2, larger values of ϵ correspond to smaller y_a and y_b, which in turn give larger ratios m_2/y_b and m_1/y_a. In our phenomenological picture this means that production of the inclusive particle (m_1) and its counterpart (m_2) is a result of fragmentation from larger masses which mimic in a sense processes with prompt resonances. The contribution to soft and hard particles from prompt resonances is different. This is reflected by different values of the momentum fraction y_a which carries the inclusive particle. The fraction y_a increases with the transverse momentum p_T. The creation of soft particles from prompt resonances is characterized by small values of y_a. Hard particles carry substantially larger fractions y_a of the momenta of their ancestors which may be resonances produced directly in the constituent interaction. In this way, the degree of increase of y_a with p_T, governed by the parameter ϵ, simulates partially creation of prompt resonances and their relative contribution to soft and hard particles. On the other hand the constant m_2 does not depend on p_T and represents minimal effective mass needed for conservation of quantum numbers in the reaction channels under consideration. Values of these parameters are determined in accordance with the experiment and are discussed in the next sections.

B. Scaling variable z and scaling function $\psi(z)$

The self-similarity of hadron interactions reflects a property that hadron constituents and their interactions are similar. This is connected with the dropping of certain dimensional quantities out of the description of physical phenomena. The self-similar solutions are constructed in terms of the self-similarity parameters. We search for a solution

$$\psi(z) = \frac{1}{N\sigma_{\text{inel}}}\frac{d\sigma}{dz} \tag{18}$$

depending on a single self-similarity variable z. Here σ_{inel} is an inelastic cross section of the reaction (1) and N is an average particle multiplicity. The variable z is a specific dimensionless combination of quantities which characterize particle production in high energy inclusive reactions. It depends on momenta and masses of the colliding and inclusive particles, structural parameters of the interacting objects, and dynamical characteristics of the produced system. We define the self-similarity variable z as follows

$$z = z_0\Omega^{-1}, \tag{19}$$

where

$$z_0 = \frac{s_\perp^{1/2}}{(dN_{ch}/d\eta|_0)^c \cdot m} \tag{20}$$

and Ω is given by Eq. (6). For a given reaction (1), the variable z is proportional to the transverse kinetic energy $s_\perp^{1/2}$ of the constituent subprocess (4) consumed on the production of the inclusive particle (m_1) and its counterpart (m_2). The energy $s_\perp^{1/2}$ is determined by the formula

$$s_\perp^{1/2} = T_a + T_b, \tag{21}$$

where

$$T_a = y_a(s_\lambda^{1/2} - M_1\lambda_1 - M_2\lambda_2) - m_1, \tag{22}$$

$$T_b = y_b(s_\chi^{1/2} - M_1\chi_1 - M_2\chi_2) - m_2. \tag{23}$$

For more details see Appendix B. The terms

$$s_\lambda^{1/2} = \sqrt{(\lambda_1 P_1 + \lambda_2 P_2)^2}, \qquad s_\chi^{1/2} = \sqrt{(\chi_1 P_1 + \chi_2 P_2)^2} \tag{24}$$

represent the energy for production of the scattered constituent and its recoil, respectively. The quantity $dN_{ch}/d\eta|_0$ is the multiplicity density of charged particles produced in the central region of the reaction (1) at the pseudorapidity $\eta = 0$. The average total charged multiplicity densities for inelastic collisions have been used in (20) for all particle species in the case of nonbiased events. They are a known function of the collision energy $\sqrt{s}$. For events with various selection criteria the multiplicity densities $dN_{ch}/d\eta|_0$ of all charged particles in the expression (20) depend on trigger. Their values corresponding to spectra with different multiplicity biases were taken from literature. The multiplicity density in the central interaction region is related to a state of the produced medium in the colliding system. The parameter c characterizes properties of this medium. It is determined from multiplicity dependence of inclusive spectra. The mass constant m is arbitrary and we fix it at the value of nucleon mass.

The scaling function $\psi(z)$ is expressed in terms of the experimentally measured inclusive invariant cross section $Ed^3\sigma/dp^3$, the multiplicity density $dN/d\eta$, and the total inelastic cross section σ_{inel}. Exploiting the definition (18) one can obtain the expression

$$\psi(z) = -\frac{\pi s A_1 A_2}{(dN/d\eta)\sigma_{\text{inel}}} J^{-1} E\frac{d^3\sigma}{dp^3}, \tag{25}$$

where s is the square of the center-of-mass energy of the corresponding NN system, A_1 and A_2 are atomic weights, and

$$J = \frac{\partial z}{\partial \kappa_1}\frac{\partial \eta}{\partial \kappa_2} - \frac{\partial z}{\partial \kappa_2}\frac{\partial \eta}{\partial \kappa_1} \tag{26}$$

is the corresponding Jacobian (see Appendix B). The Jacobian depends on kinematic variables characterizing the inclusive process (1). The multiplicity density $dN/d\eta$ in the expression (25) concerns particular hadrons species. It depends on the center-of-mass energy, on various multiplicity selection criteria, and also on the production angles at which the inclusive spectra were measured. The procedure of obtaining the corresponding values of $dN/d\eta$ from the p_T spectra is described in Appendix B. The function $\psi(z)$ is normalized as follows

$$\int_0^\infty \psi(z)dz = 1. \tag{27}$$

The above relation allows us to interpret the function $\psi(z)$ as a probability density to produce an inclusive particle with the corresponding value of the variable z.

III. PROPERTIES OF THE SCALING FUNCTION $\psi(z)$

Let us investigate properties of z presentation of experimental data obtained in proton-proton collisions at high energies.

A. Energy independence of $\psi(z)$

We have analyzed experimental data [20–28] on inclusive hadron ($h^\pm$, π^-, K^-, and $\bar{p}$) production in minimum-biased proton-proton collisions. The data on inclusive cross sections were measured in the central rapidity region at FNAL, ISR, and RHIC energies $\sqrt{s}$ = 19–200 GeV.

The energy dependence of the charged hadron spectra on the transverse momentum is shown in Fig. 2(a). The distributions cover the range up to $p_T \simeq 10$ GeV/c. The cross sections change within the range of 12 orders of magnitudes. The strong dependence of the spectra on the collision energy $\sqrt{s}$ increases with transverse momentum. Figure 2(b) shows the z-presentation of the same data. The scaling variable z depends on the average multiplicity density of charged particles produced in the central pseudorapidity region of the collision. We have used experimentally measured values of $dN_{ch}/d\eta|_{\eta=0}$ [29] for minimum-biased collisions in the analysis of energy and angular properties of $\psi(z)$. The independence of the scaling function $\psi(z)$ on the collision energy $\sqrt{s}$ is found for the constant values of the parameters $c = 0.25$, $\delta = 0.5$, and $\epsilon = 0.2$. The form of $\psi(z)$ manifests two regimes of particle production. The hard regime is characterized by the power law $\psi(z) \sim z^{-\beta}$ for large z. Soft processes correspond to the behavior of $\psi(z)$ for small z. The slope of the scaling curve decreases with z in this region.

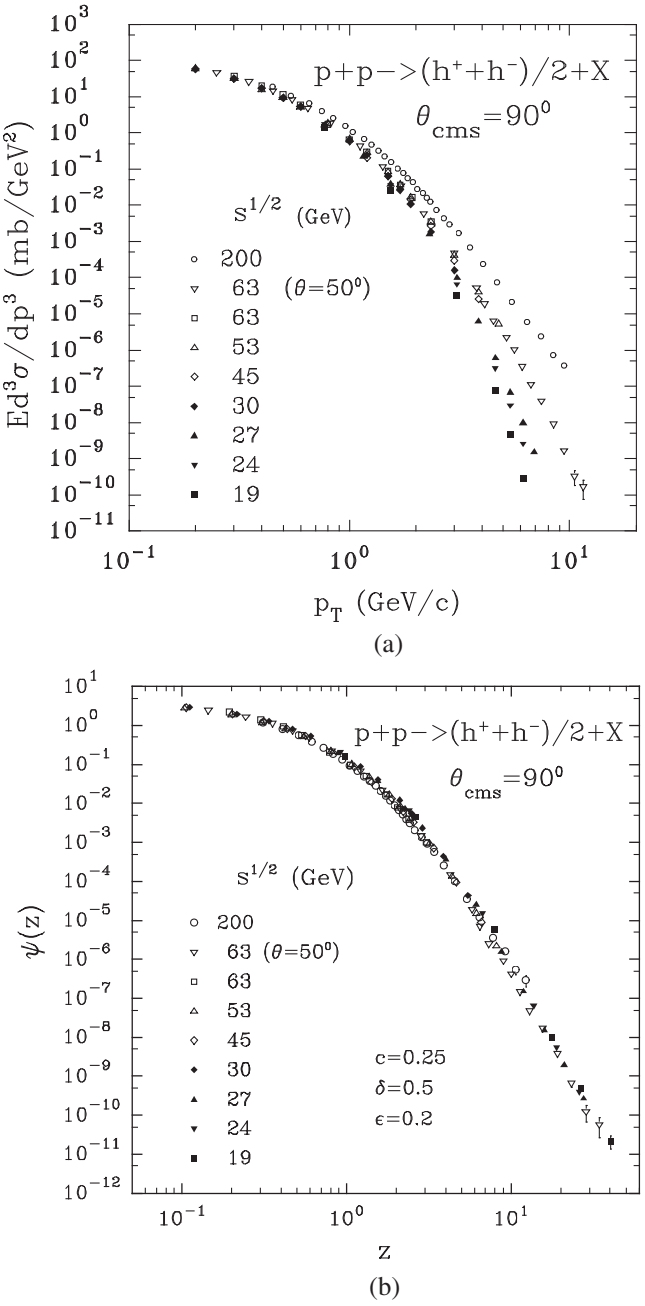

FIG. 2. (a) Transverse momentum spectra of the charged hadrons produced in pp collisions at $\sqrt{s}$ = 19–200 GeV. Experimental data are taken from Refs. [20,21,23,25]. (b) The corresponding scaling function $\psi(z)$.

The invariant cross sections for the π^--meson production as a function of the collision energy and transverse momentum are plotted in Fig. 3(a). The spectra were measured over a wide transverse momentum range p_T = 0.1–10 GeV/c. The cross sections change from 10^2 to 10^{-10} mb/GeV^2. The strong dependence of the pion spectra on $\sqrt{s}$ was observed in analogy with the case of the

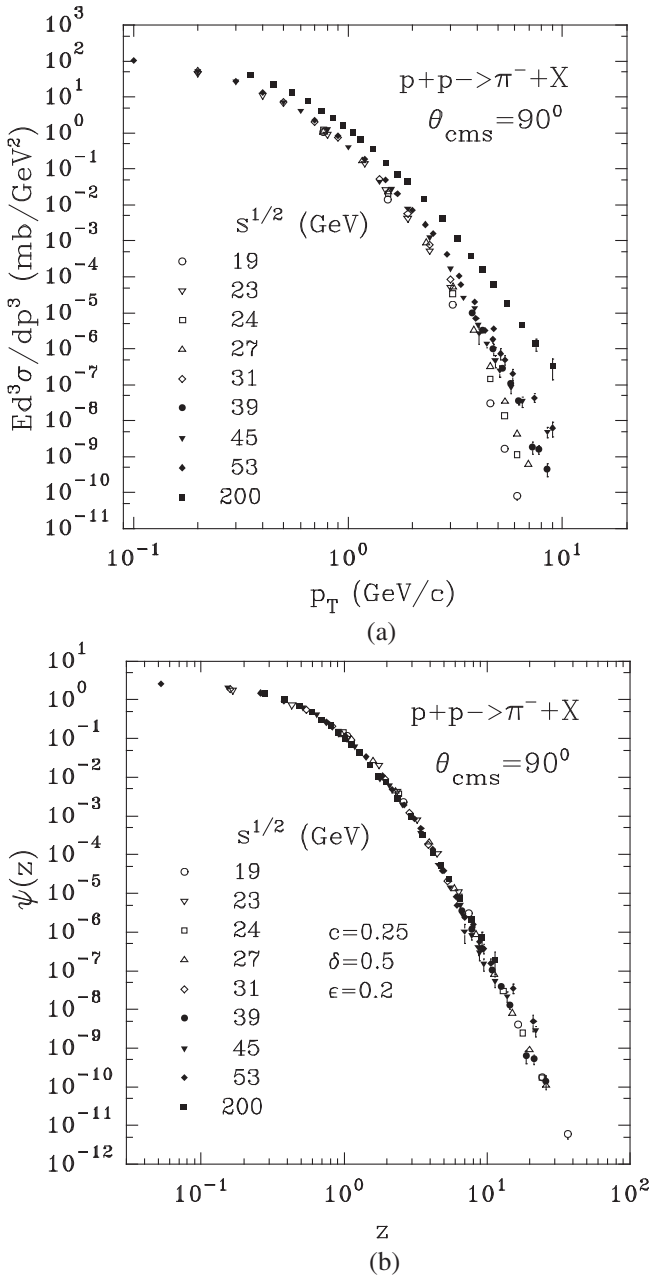

FIG. 3. (a) Transverse momentum spectra of the π^--mesons produced in pp collisions at $\sqrt{s} = 19$–200 GeV. Experimental data are taken from Refs. [20,21,24,26]. (b) The corresponding scaling function $\psi(z)$.

charged hadron production. The z presentation of the same data is shown in Fig. 3(b). For pions (as well as for all other types of the particles—kaons, antiprotons, ...) the dependence of z on the charged particle multiplicity density $dN_{ch}/d\eta|_{\eta=0}$ has been used in the formula (20). On the other hand, the scaling function (25) is normalized to the multiplicity density of pions. Independence of the scaling function for pions on $\sqrt{s}$ was obtained for $c = 0.25$, $\delta = 0.5$, and $\epsilon = 0.2$, as well as for the charged hadrons. The shape of $\psi(z)$ is found to be the same in both cases.

Transverse momentum spectra for the K^--meson production are shown in Fig. 4(a). The cross sections were measured in the range $p_T = 0.1$–8 GeV/c. The data [28] for the K^0_s-mesons obtained by the STAR Collaboration at RHIC are also presented in Fig. 4(a). The K-meson spectra demonstrate the strong dependence on the collision energy $\sqrt{s}$. The corresponding scaling function $\psi(z)$ is depicted in Fig. 4(b). The independence of $\psi(z)$ on $\sqrt{s}$ is restored for $c = 0.25$, $\delta = 0.5$, and $\epsilon = 0.3$. The similar features of the

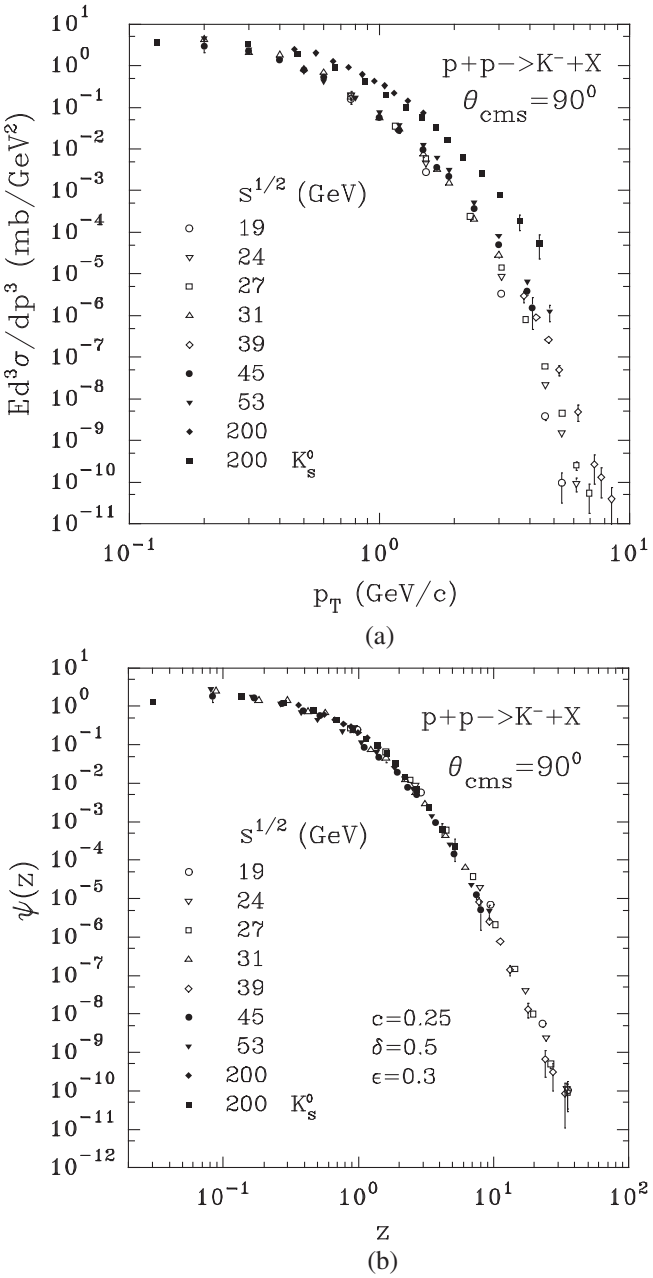

FIG. 4. (a) Transverse momentum spectra of the K^--mesons produced in pp collisions at $\sqrt{s} = 19$–200 GeV. The spectrum of K^0_s-mesons is shown by filled squares (■). Experimental data are taken from Refs. [20,21,24,27,28]. (b) The corresponding scaling function $\psi(z)$.

p_T and z presentations of experimental data [20,21,24,27] on the antiproton production are presented in Figs. 5(a) and 5(b). The energy independence of $\psi(z)$ for antiprotons was established for $c = 0.25$, $\delta = 0.5$, and $\epsilon = 0.35$.

Based on the obtained results we can conclude that the energy independence of the scaling function $\psi(z)$ is valid for different types of hadrons in a wide range of the center-of-mass energy $\sqrt{s}$ and the transverse momentum p_T.

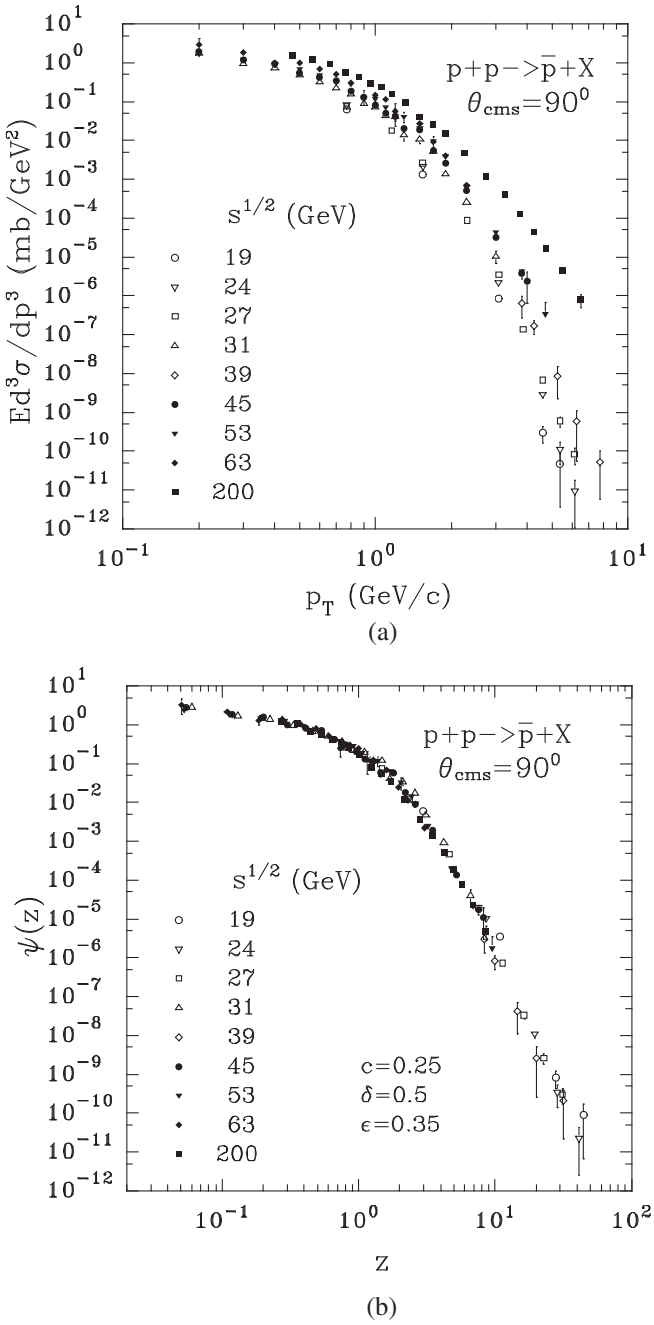

FIG. 5. (a) Transverse momentum spectra of the antiprotons produced in pp collisions at $\sqrt{s} = 19$–200 GeV. Experimental data are taken from Refs. [20,21,24,27]. (b) The corresponding scaling function $\psi(z)$.

B. Angular independence of $\psi(z)$

We have analyzed experimental data [21,30] on the angular dependence of negative hadrons (pions, kaons, and antiprotons) measured at ISR energies. The data were obtained in the central and fragmentation regions. Results of our analysis are demonstrated at the energy $\sqrt{s} = 53$ GeV.

Invariant cross sections for the π^--meson production as a function of the center-of-mass angle θ and the transverse momentum p_T are shown in Fig. 6(a). The angles cover the range $\theta = 3°$–$90°$. The central and fragmentation regions are distinguished by a different behavior of differential cross sections. The z presentation of the same data is shown in Fig. 6(b). The total charged hadron multiplicity density $dN_{ch}/d\eta|_{\eta=0}$ represents an angular independent factor in the definition of the variable z. Contrary to this, the scaling function (25) is normalized to the multiplicity density $dN/d\eta$ of pions depending on the angle θ. The angular and energy independence of the scaling function for pions was obtained for the same values of $c = 0.25$, $\delta = 0.5$, and $\epsilon = 0.2$. Let us remark that the function $\psi(z)$ is sensitive to the value of m_2 for small θ. This parameter is determined from the corresponding exclusive reaction

$$p + p \rightarrow \pi^- + p + p + \pi^+. \tag{28}$$

The above reaction is a limiting case of the subprocess (4) for $x_1 = x_2 = y_a = y_b = 1$. From Eqs. (5) and (28) we get $m_2 = m(\pi^+) = 0.14$ GeV. This value was used in our analysis for the inclusive π^--meson production.

Transverse momentum spectra for the K-mesons and antiprotons produced in pp collisions at different angles are shown in Figs. 7(a) and 8(a). In addition to the ISR data at $\sqrt{s} = 53$ GeV, the data from RHIC at $\sqrt{s} = 200$ GeV are also shown. The angular dependence of the spectra demonstrates a strong difference between the central and fragmentation regions. The corresponding function $\psi(z)$ for kaons and antiprotons is plotted in Figs. 7(b) and 8(b), respectively. For both particles, the charged hadron multiplicity density $dN_{ch}/d\eta|_{\eta=0}$ represents an angular independent factor in the definition of the variable z. The scaling function (25) is normalized to the angular dependent multiplicity density $dN/d\eta$ of kaons and antiprotons, respectively.

The independence of $\psi(z)$ on the angle θ is obtained for $c = 0.25$, $\delta = 0.5$, and $\epsilon = 0.3$ for kaons and for $c = 0.25$, $\delta = 0.5$, and $\epsilon = 0.35$ for antiprotons. The values of these parameters allowed us to obtain simultaneously the angular and energy independence of the scaling function. Analogous to the case of π^--mesons, the function $\psi(z)$ for kaons and antiprotons is sensitive to the value of m_2 at small angles θ. The corresponding values of the parameter m_2 are determined from the exclusive reactions

$$p + p \rightarrow K^- + p + p + K^+, \tag{29}$$

$$p + p \to \bar{p} + p + p + p. \quad (30)$$

Using Eq. (5) for $x_1 = x_2 = y_a = y_b = 1$ and Eqs. (29) and (30), we get $m_2 = m(K^+) = 0.5$ GeV and $m_2 = m(p) = 0.94$ GeV for the inclusive production of the K^--mesons and antiprotons, respectively.

The new data [31] on the angular dependence of the transverse momentum spectra of charged hadrons obtained by the BRAHMS Collaboration at RHIC are shown in Fig. 9(a). The data cover a wide range of the center-of-mass angles ($\theta = 5°$–$90°$) and the transverse momenta ($p_T = 0.25$–5.65 GeV/c) of the produced hadrons at the collision energy $\sqrt{s} = 200$ GeV. As seen from Fig. 9(a),

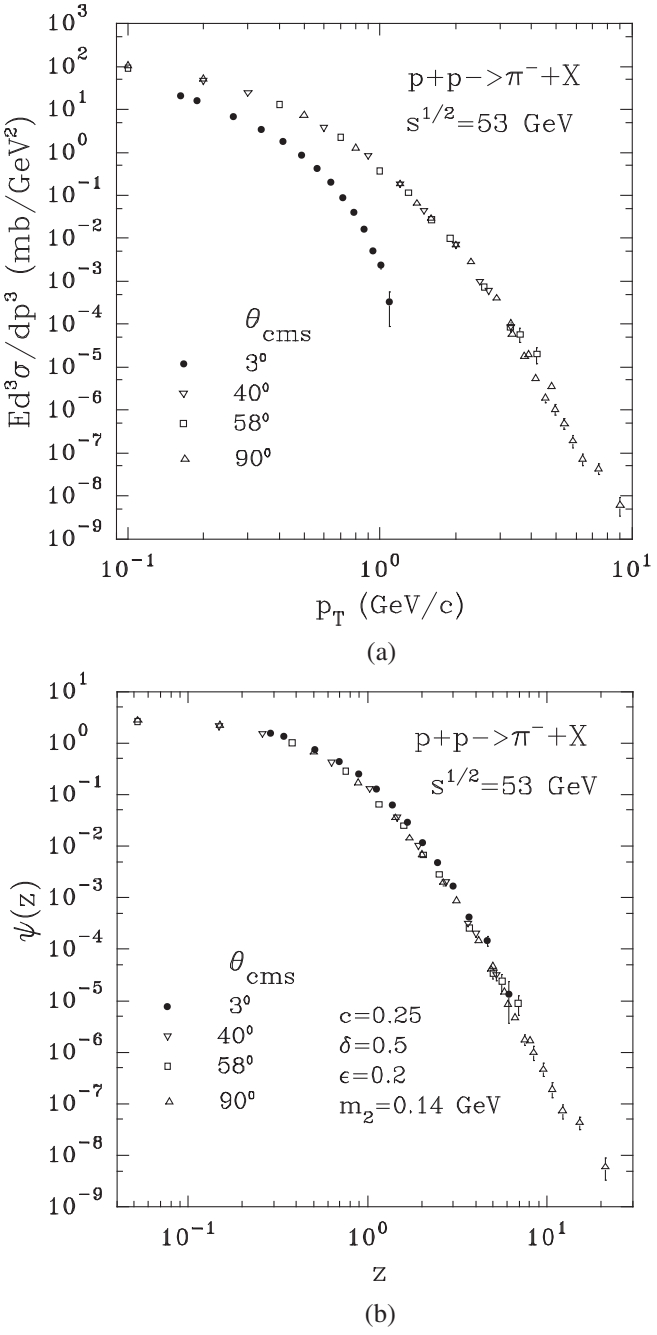

FIG. 6. (a) Transverse momentum spectra of the π^--mesons produced in pp collisions for different angles at $\sqrt{s} = 53$ GeV. Experimental data are taken from Refs. [21,30]. (b) The corresponding scaling function $\psi(z)$.

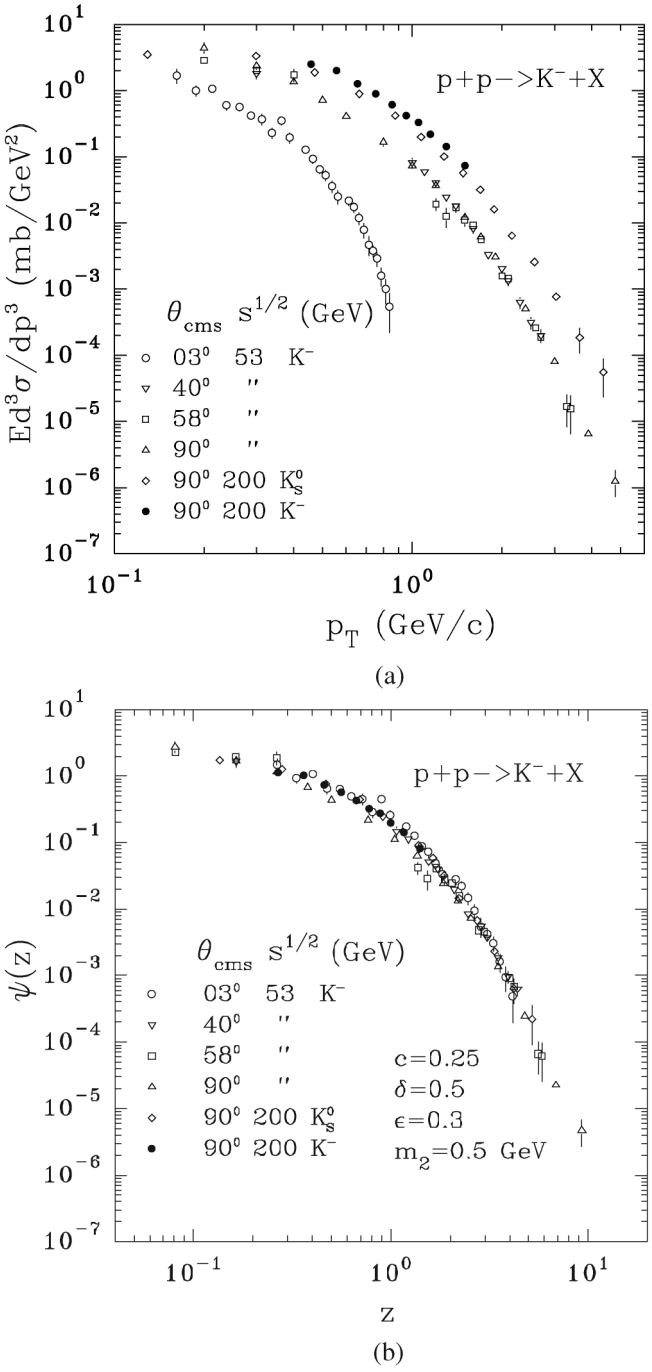

FIG. 7. (a) Transverse momentum spectra of the K^--mesons produced in pp collisions for different angles at $\sqrt{s} = 53$ GeV. The K^- and K^0_s-meson spectra for $\theta_{\rm cms} \simeq 90°$ at $\sqrt{s} = 200$ GeV are shown by a filled circle (●) and diamond (◇), respectively. Experimental data are taken from Refs. [21,27,28,30]. (b) The corresponding scaling function $\psi(z)$.

the difference between the spectra for $\theta = 5^0$ and $\theta = 90°$ enhances with the transverse momentum and reaches the order of magnitude at $p_T = 3$ GeV/c. For low $p_T < 1$ GeV/c more systematic study of the angular dependence of the spectra is needed to establish reliably the behavior of $\psi(z)$ in the range. The z-presentation of the data [see Fig. 9(b)] demonstrates the angular independence of the

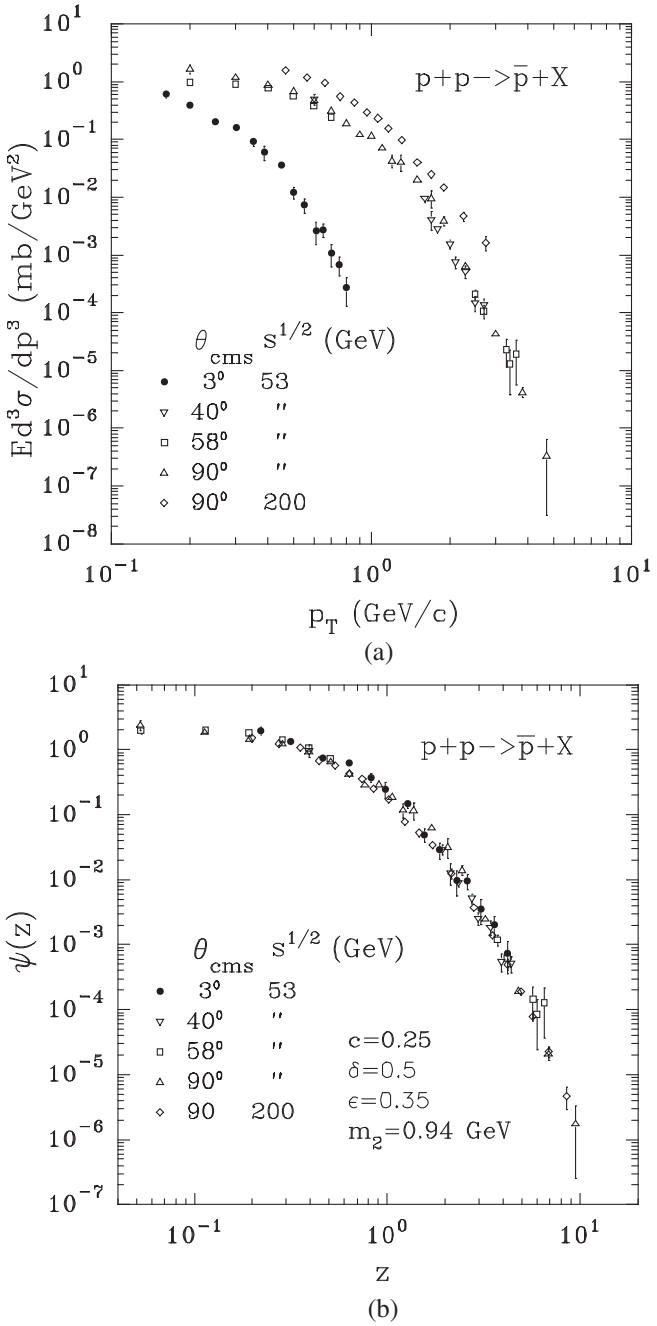

FIG. 8. (a) Transverse momentum spectra of the antiprotons produced in pp collisions for different angles at $\sqrt{s} = 53$ GeV. The antiproton spectrum for $\theta_{\rm cms} \simeq 90°$ at $\sqrt{s} = 200$ GeV is shown using diamonds ($\diamond$). Experimental data are taken from Refs. [21,27,30]. (b) The corresponding scaling function $\psi(z)$.

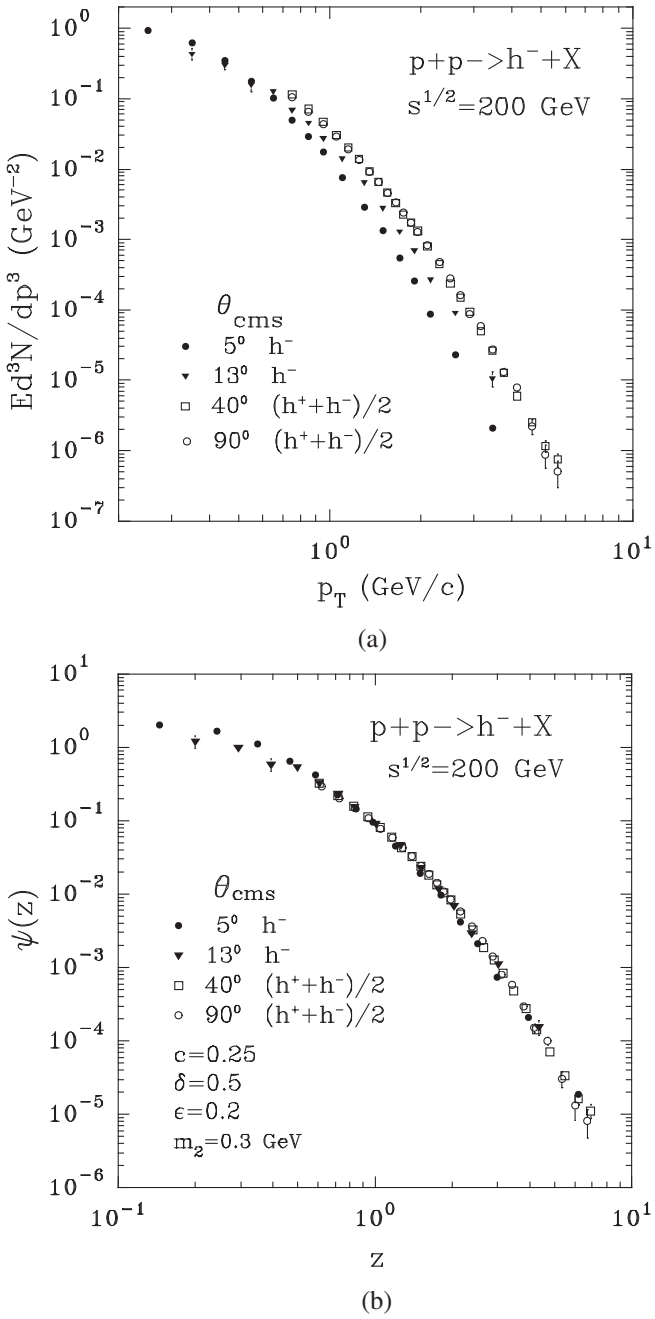

FIG. 9. (a) Transverse momentum spectra of the charged hadrons produced in pp collisions for different angles at $\sqrt{s} = 200$ GeV. Experimental data are taken from Ref. [31]. (b) The corresponding scaling function $\psi(z)$.

scaling function for the same parameters $c = 0.25$, $\delta = 0.5$, $\epsilon = 0.2$, and $m_2 = 0.3$ GeV as found in the case of the charged hadrons at lower energies $\sqrt{s} = 19$–63 GeV.

C. Multiplicity independence of $\psi(z)$

The STAR Collaboration obtained the new data [32] on the multiplicity dependence of the inclusive spectra of charged hadrons produced in pp collision in the central

rapidity range $|\eta| < 0.5$ at the energy $\sqrt{s} = 200$ GeV. The transverse momentum distributions were measured up to 9.5 GeV/c using different multiplicity selection criteria. Figure 10(a) demonstrates a strong dependence of the spectra on the multiplicity density at $dN_{ch}/d\eta = 2.5$, 6.0, and 8.0. The same data are shown in Fig. 10(b) in the scaling form. The scaling function $\psi(z)$ changes over 6 orders of magnitude in the range of $z = 0.2$–10. The independence of $\psi(z)$ on the multiplicity density $dN_{ch}/d\eta$ was obtained. The result provides a restriction on the parameter c. We have found its value to be $c = 0.25$.

The STAR Collaboration measured the multiplicity dependence of the K^0_S-meson and Λ-baryon spectra [33] in the central rapidity range $|\eta| < 0.5$ at the energy

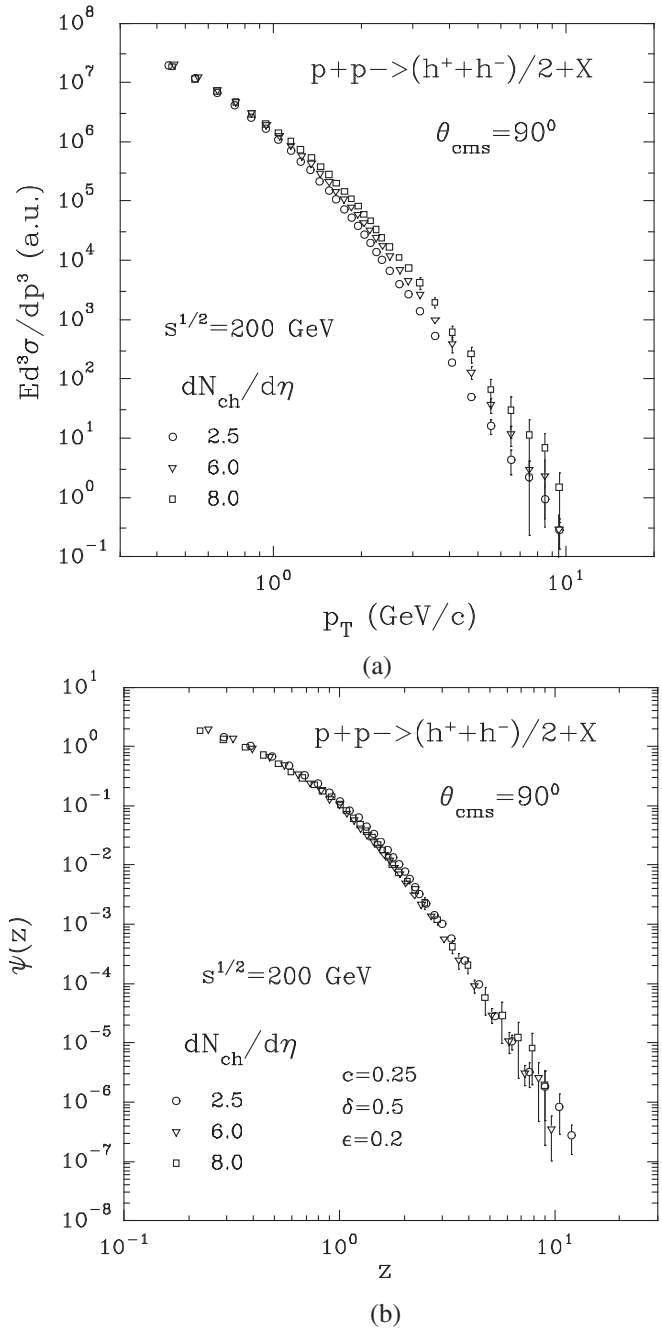

FIG. 10. (a) Transverse momentum spectra of the charged hadrons produced in pp collisions for different multiplicity densities at $\sqrt{s} = 200$ GeV. The spectra are normalized at $p_T = 0.4$ GeV/c. Experimental data are taken from Ref. [32]. (b) The corresponding scaling function $\psi(z)$.

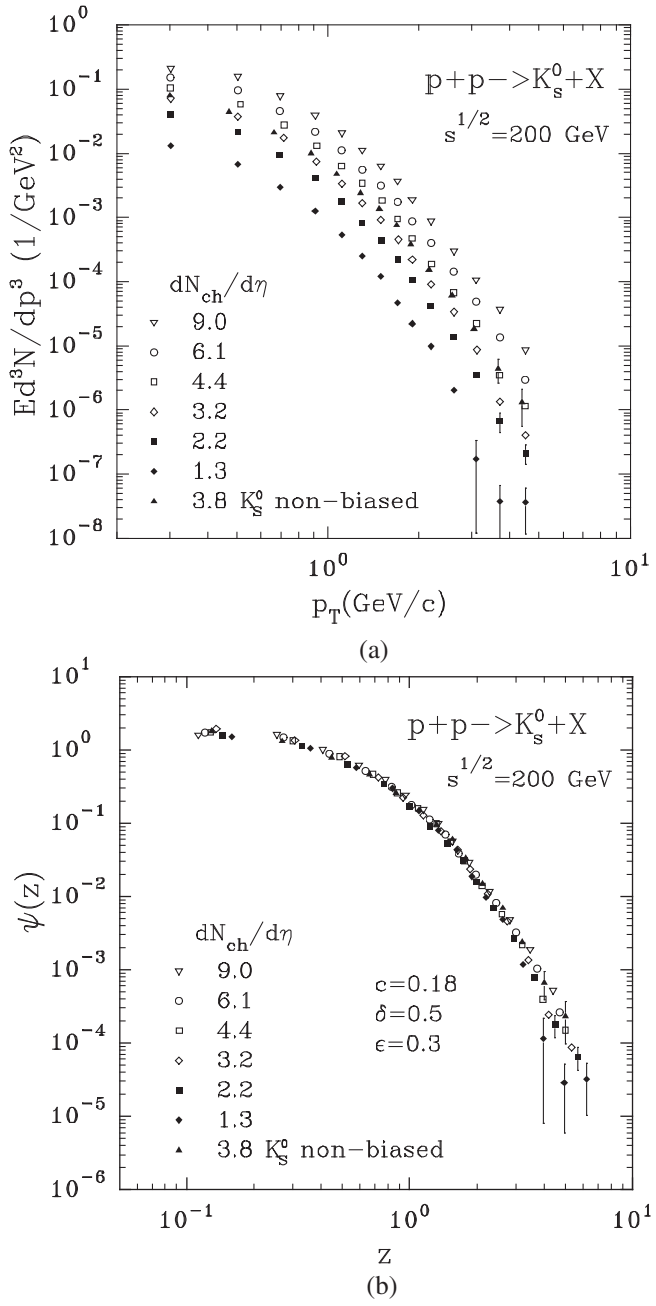

FIG. 11. (a) Transverse momentum spectra of the K^0_s-mesons produced in pp collisions for different multiplicity densities at $\sqrt{s} = 200$ GeV. The K^0_s-meson spectrum for nonbiased pp collisions at $\sqrt{s} = 200$ GeV is shown by filled triangles (▲). Experimental data are taken from Ref. [28,33]. (b) The corresponding scaling function $\psi(z)$.

$\sqrt{s} = 200$ GeV as well. The spectra are presented in Figs. 11(a) and 12(a). The charged multiplicity density was varied in the range $dN_{ch}/d\eta = 1.3$–9.0. The transverse momentum distributions were measured up to 4.5 GeV/c. The corresponding function $\psi(z)$ is shown in Figs. 11(b) and 12(b), respectively. The scaling behavior

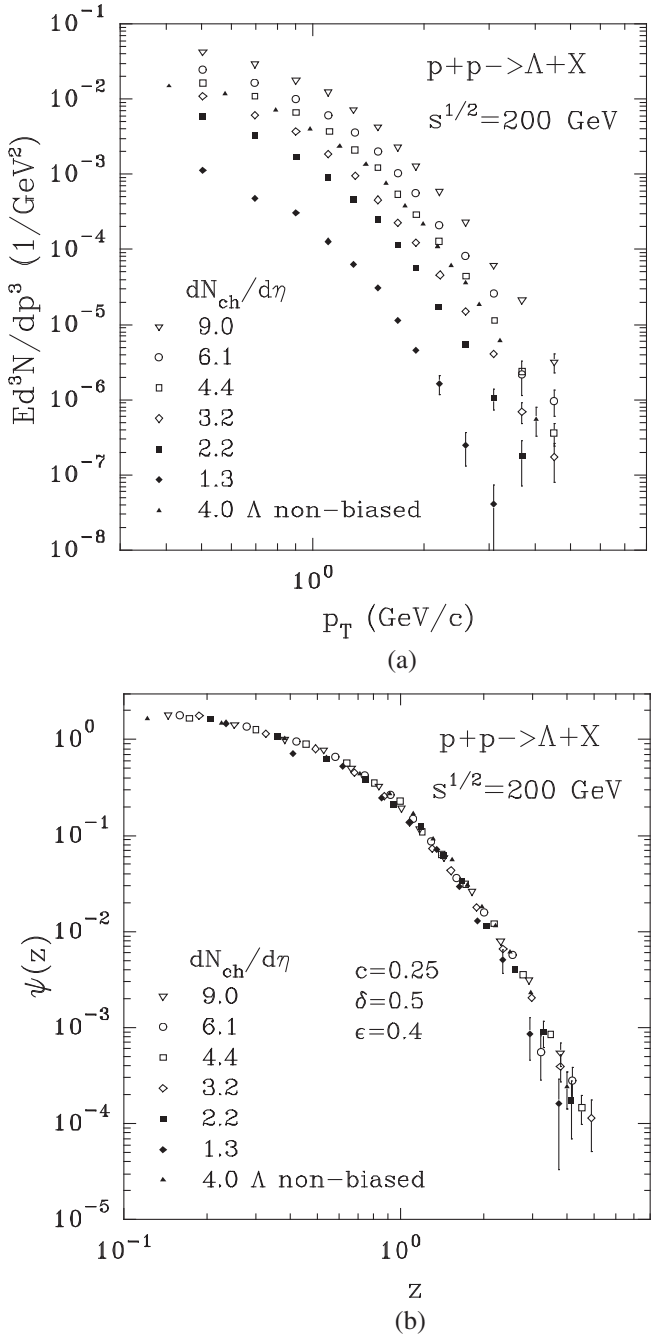

FIG. 12. (a) Transverse momentum spectra of the Λ-baryons produced in pp collisions for different multiplicity densities at $\sqrt{s} = 200$ GeV. The Λ-baryon spectrum for nonbiased pp collisions at $\sqrt{s} = 200$ GeV is shown by filled triangles (▲). Experimental data are taken from Ref. [28,33]. (b) The corresponding scaling function $\psi(z)$.

provides a strong restriction on the value of c. The data favor $c = 0.25$ in both cases.

We conclude that the analyzed experimental data on the multiplicity dependence of the spectra of the charged hadrons, the K^0_S-mesons, and Λ-baryons produced in pp collisions at RHIC confirm the generalized z-scaling and indicate to the same value of the parameter c.

D. Flavor independence of $\psi(z)$

Flavor independence of z-scaling was studied in Ref. [34]. It was shown that the value of the slope parameter β of the scaling function $\psi(z)$ at high z is the same for different types of produced hadrons (π, K, $\bar{p}$). The hypothesis was supported by results of the analysis of hadron ($\pi^{\pm,0}$, K, $\bar{p}$) spectra for high p_T in pp and pA collisions.

The proposed generalization of the z-scaling provides a unified description of the spectra of different hadrons over a wide z-range. This includes both the large z region corresponding to hard processes and the low z-region characteristic for soft interactions. Restoration of the energy, angular, and multiplicity independence of the z-presentation of experimental data gives the same shape of the scaling function for different particle species. Exploiting the property (A10), the scaling functions corresponding to p_T spectra of negative pions, kaons, antiprotons, and $\Lambda's$ can be reduced to a single curve. This is illustrated in Fig. 13 where the transverse momentum distributions of different hadrons produced in pp collisions are shown in the unified form. It is important to stress that the result is based on p_T distributions which reveal strong dependence on energy, angle, multiplicity, and type of the produced particle. The data cover a wide range of collision

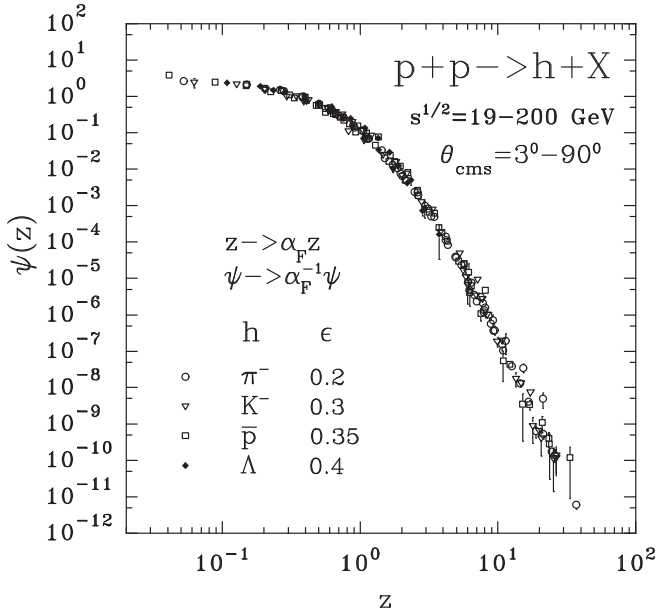

FIG. 13. Flavor independence of z-scaling. The spectra of π, K, $\bar{p}$, and Λ produced in pp collisions in z presentation.

energy, transverse momentum, and angle of detection. The same applies to the pp reactions with various multiplicity selection criteria connected with different centralities.

In conclusion, the analyzed spectra of negative pions, kaons, antiprotons, and $\Lambda's$ can be described by a single function $\psi(z)$. This is achieved by the transformation $z \rightarrow \alpha_F \cdot z$ and $\psi \rightarrow \alpha_F^{-1} \cdot \psi$ which does not change the shape of $\psi(z)$ in the log-log plot. The factor α_F is a constant independent of kinematical variables ($\sqrt{s}$, p_T, and θ). The mechanism of hadron production on the level of inclusive cross sections can be characterized by the universal function $\psi(z)$ and by the parameters δ, ϵ, and c. In the proposed scheme, the production of different hadrons in high energy proton-proton collisions is parametrized by different values of ϵ. We assume that this phenomenological parameter has a deep internal connection to the processes of formation of individual hadrons. The obtained results give strong support for the assumption that flavor independence of the scaling function $\psi(z)$ over a wide z-range would also be valid for secondary particles with heavy flavor content.

IV. HADRON SPECTRA IN NLO QCD AND z-PRESENTATION

Here we present results of the next-to-leading order (NLO) QCD calculations of inclusive cross sections of hadrons over a wide range of collision energy (up to the LHC energy) and transverse momentum. The dependence of the spectra in p_T and z presentations on the collision energy, angle of produced particles for different parton distribution, and fragmentation functions (PDFs, and FFs) are studied. The sensitivity of the results to the choice of the renormalization (μ_R), initial-state factorization (μ_F), and final-state factorization (fragmentation) (μ_H) scales is verified.

In the paper we use the code from Aversa-Chiappetta-Greco-Guillet [35] of the NLO QCD production of high transverse momentum hadrons. The inclusive differential cross section for the production of a single hadron ($h^{\pm}$, π, K, ...) with the transverse momentum p_T and the pseudorapidity η is written as follows

$$d^2\sigma^h/d\vec{p}_T^2 d\eta = \sum_{i,j,k} \int dx_1 dx_2 f_{i/h_1}(x_1, \mu_F) \cdot f_{j/h_2}(x_2, \mu_F) \times [(\alpha_S(\mu_R)/2\pi)^2 \cdot d^2\hat{\sigma}_{ij,k}/d\vec{p}_T^2 d\eta + (\alpha_S(\mu_R)/2\pi)^3 \cdot K_{ij,k}(\mu_R, \mu_F, \mu_H)] dz/z^2 \cdot D_k^h(z, \mu_H). \quad (31)$$

The function $f_{i/h_1}(x_1, \mu_F)$ describes the distribution of a parton i in the hadron h_1 on the momentum fraction x_1 at the factorization scale μ_F. The fragmentation of a parton k into the hadron h is described by the function $D_k^h(z, \mu_H)$. The parton momentum fraction carried by the hadron h at the fragmentation scale μ_H is equal to z. The cross section terms in the LO and NLO QCD are described by $d^2\hat{\sigma}_{ij,k}/d\vec{p}_T^2 d\eta$ and $K_{ij,k}$, respectively. The $\overline{\text{MS}}$ scheme is used to subtract final-state collinear singularities. The strong coupling $\alpha_S(\mu_R)$ is defined in the $\overline{\text{MS}}$ renormalization scheme at the scale μ_R. The parton distribution functions CTEQ [36] and MRST [37] and the fragmentation functions KKP [38] and BKK [39] were used in the calculations.

The invariant cross sections for the charged hadron production as a function of the collision energy $\sqrt{s}$ and transverse momentum p_T calculated in the NLO QCD are shown in Fig. 14(a). The calculations depicted by the dashed lines were performed with the parton distribution functions CTEQ5m and the fragmentation functions KKP. The renormalization, factorization, and fragmentation scales were set to be equal to each other $\mu_R = \mu_F = \mu_H = c \cdot p_T$ and $c = 1$. The spectra were calculated over a wide range of the transverse momentum $p_T =$ 1–100 GeV/c and the energy $\sqrt{s} =$ 23–14 000 GeV at $\theta_{cms} = 90°$. As seen from Fig. 14(a) the strong dependence of the spectra on the collision energy increases with p_T. The difference of the cross sections at $\sqrt{s} = 23$ and 14 000 GeV reaches about 5 and 8 orders of magnitude at $p_T = 5$ and 10 GeV/c, respectively. Experimental data on cross sections obtained at FNAL [20], CERN [23], and BNL [25] are shown in Fig. 14(a) by a triangle ($\triangle$), plus sign (+), and circle ($\circ$), respectively. The same data are plotted in the dependence on the variable z in Fig. 14(b). The solid line represents asymptotic behavior of the scaling function $\psi(z)$ (at constant value of the slope parameter) for high z. The z presentation of the NLO QCD calculations of the charged hadron spectra is shown by the dashed curves. Because data on multiplicity densities are not available in the TeV energy region, the NLO QCD calculations were normalized at $z = 1$ following the procedure described in Appendix B. A reasonable agreement between experimental data and the corresponding NLO QCD calculations presented in the framework of the z-scaling is observed. One can see, however, that the NLO QCD predictions demonstrate dramatic deviation from the asymptotic behavior predicted by z-scaling as the collision energy and transverse momentum increase in the region where experimental measurements are not performed yet.

Figures 15 and 16 show p_T and z presentations of the inclusive spectra of π and K mesons produced in pp collisions over a range $p_T =$ 1–100 GeV/c, $\sqrt{s} =$ 30–14 000 GeV, and $|\eta| < 0.35$. The NLO QCD calculations with the CTEQ5m parton densities and KKP fragmentation functions are plotted by the dashed lines. Experimental data are depicted by points [triangle ($\triangle$), plus sign (+), and circle ($\circ$)]. The results shown in Figs. 14–16 demonstrate that general features of both presentations are independent of the type of the produced hadron ($h^{\pm}$, π, K). The z presentation of the NLO QCD calculated results indicate considerable deviation from the

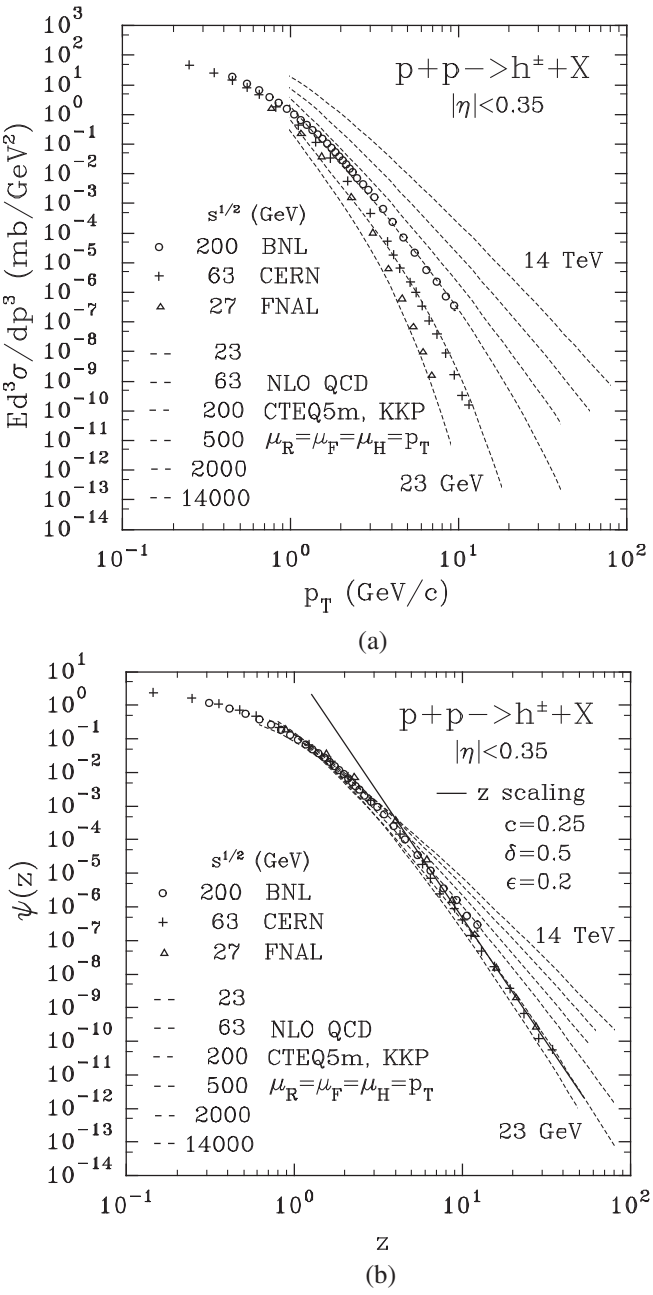

FIG. 14. The NLO QCD predictions of transverse momentum spectra of the charged hadrons produced in pp collisions over a range $\sqrt{s}$ = 23–14 000 GeV and $|\eta| < 0.35$ with CTEQ5m [36] parton distributions and KKP [38] fragmentation functions in p_T (a) and z (b) presentations. Experimental FNAL [20], CERN [23], and BNL [25] data are shown by a triangle (△), plus sign (+), and circle (∘), respectively. The solid line is the prediction of the asymptotic behavior of $\psi(z)$ by the z-scaling.

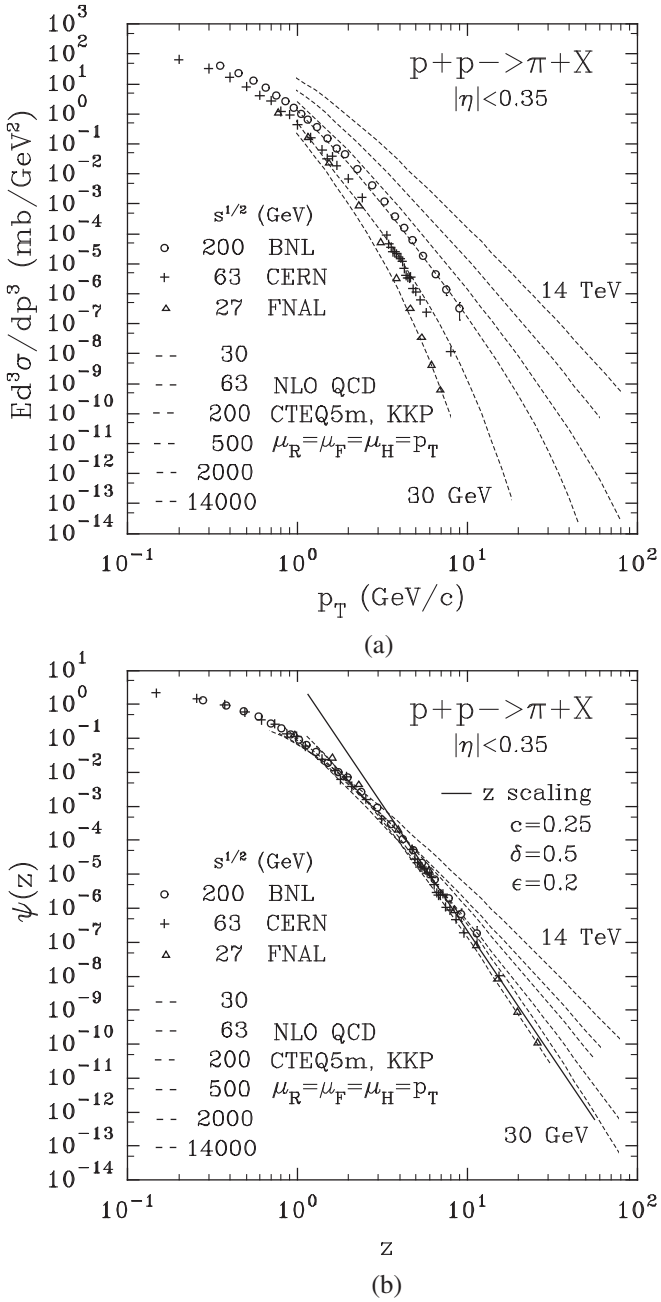

FIG. 15. The NLO QCD predictions of transverse momentum spectra of the π mesons produced in pp collisions over a range $\sqrt{s}$ = 30–14 000 GeV and $|\eta| < 0.35$ with CTEQ5m [36] parton distributions and KKP [38] fragmentation functions in p_T (a) and z (b) presentations. Experimental FNAL [20], CERN [21,22], and BNL [26] data are shown by a triangle (△), plus sign (+), and circle (∘), respectively. The solid line is the prediction of the asymptotic behavior of $\psi(z)$ by the z-scaling.

asymptotic behavior predicted by the z-scaling. A similar comparison of the angular dependence of charged hadron and π meson spectra predicted by the NLO QCD with the z-scaling results is shown in Figs. 17 and 18. In contrast to the asymptotic behavior of $\psi(z)$ (solid line) the NLO QCD curves (dashed lines) demonstrate strong dependence on the angle $\theta_{\rm cms}$ over a range 3°–90° in the z-presentation. The NLO QCD calculations with other parton (MRST)[37] and fragmentation (BKK)[39] functions as well as with the variation ($c = 1/2,\ 1,\ 2$) of the renormalization (μ_R), factorization (μ_F), and fragmentation (μ_H) scales give similar results. We would like to emphasize that

z-presentation of all calculations was performed with the same values of the parameters δ, ϵ, and c as obtained from our analysis of experimental data. The results of the analysis illustrate the qualitative and quantitative difference of the NLO QCD predictions and the z-scaling regularity at high p_T.

Based on the obtained results we conclude that self-similar features of particle production dictated by the z-scaling give strong restriction on the asymptotic behavior of the scaling function $\psi(z)$. The behavior is not reproduced by the NLO QCD evolution of cross sections with the phenomenological parton distribution and fragmentation functions used in the present analysis.

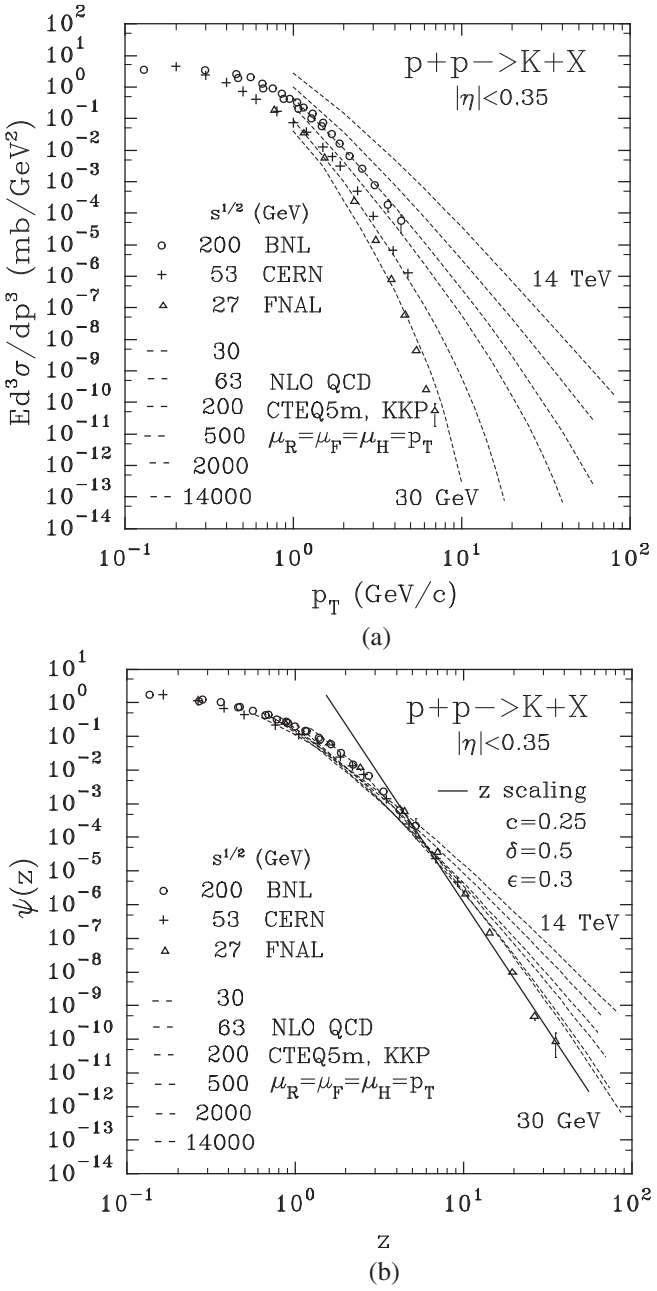

FIG. 16. The NLO QCD predictions of transverse momentum spectra of the K mesons produced in pp collisions over a range $\sqrt{s} = 30$–$14\,000$ GeV and $|\eta| < 0.35$ with CTEQ5m [36] parton distributions and KKP [38] fragmentation functions in p_T (a) and z (b) presentations. Experimental FNAL [20], CERN [21], and BNL [27,28] data are shown by a triangle ($\triangle$), plus sign (+), and circle ($\circ$), respectively. The solid line is the prediction of the asymptotic behavior of $\psi(z)$ by the z-scaling.

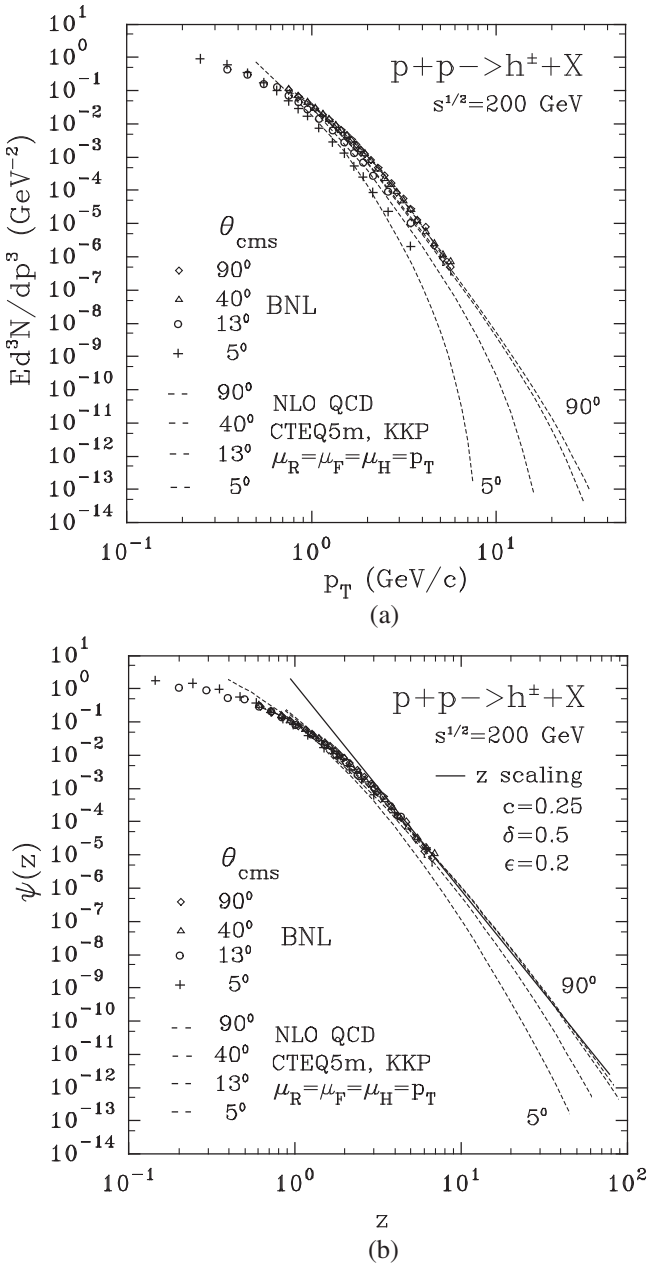

FIG. 17. The NLO QCD predictions of angular dependence of transverse momentum spectra of charged hadrons produced in pp collisions at $\sqrt{s} = 200$ GeV for $\theta_{\rm cms} = 5°$–$90°$ with CTEQ5m [36] parton distributions and KKP [38] fragmentation functions in p_T (a) and z (b) presentations. Experimental data [31] obtained at RHIC are shown by the plus sign (+), circle ($\circ$), triangle ($\triangle$), and diamond ($\diamond$). The solid line is the prediction of the asymptotic behavior of $\psi(z)$ by the z-scaling.

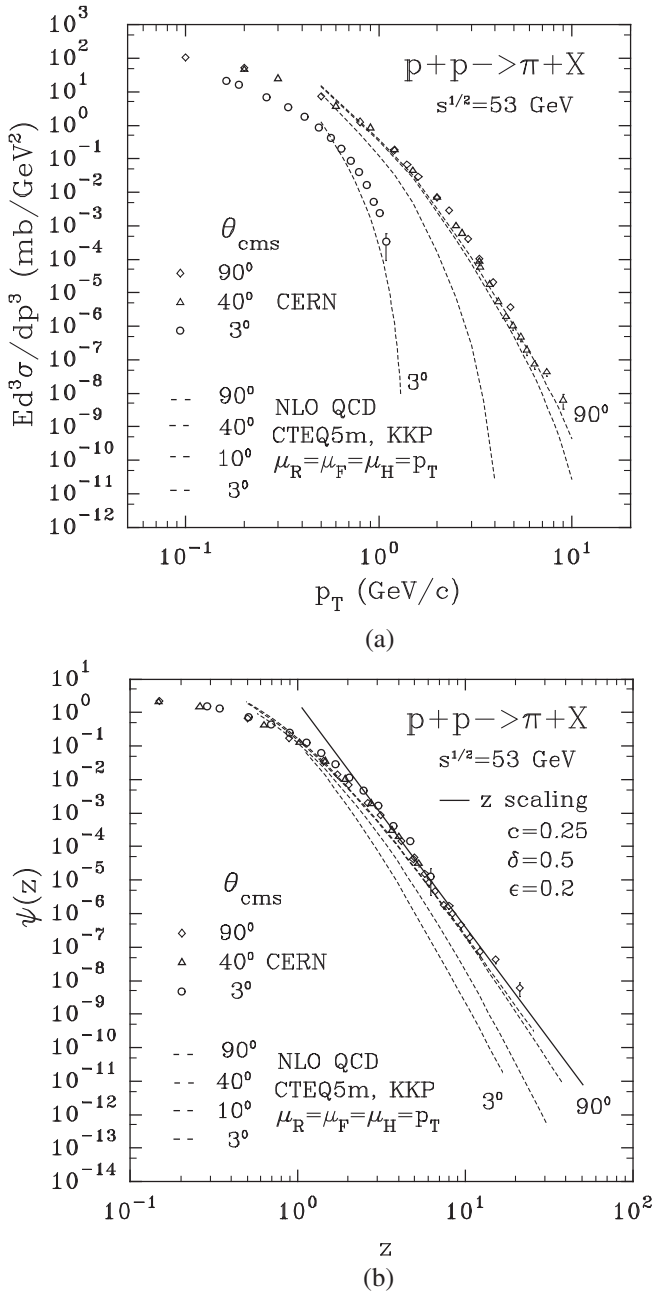

FIG. 18. The NLO QCD predictions of angular dependence of transverse momentum spectra of π mesons produced in pp collisions at $\sqrt{s} = 53$ GeV for $\theta_{\rm cms} = 3°$–$90°$ with CTEQ5m [36] parton distributions and KKP [38] fragmentation functions in p_T (a) and z (b) presentations. Experimental data [21,30] obtained at ISR are shown by the circle ($\circ$), triangle ($\triangle$), and diamond ($\diamond$). The solid line is the prediction of the asymptotic behavior of $\psi(z)$ by the z-scaling.

V. DISCUSSION

An analysis of experimental data on inclusive cross sections for different hadron species performed in z-presentation shows that the shape of the scaling function $\psi(z)$ for proton-proton collisions is the universal one. The universality means that the scaling function is the same for hadrons with different flavor content. The behavior of $\psi(z)$ is described by the power law, $\psi(z) \sim z^{-\beta}$, in the asymptotic (high-z) region. It was found however, that β is different for pp and $\bar{p}p$ collisions [18]. This holds for direct photon and jet production as well. The scaling function at high-z describes features of a hard mechanism of particle production. In the low-p_T (low-z) region corresponding to the soft regime of particle production the scaling function bends and straightens out in the logarithmic plot.

The suggested procedure for the construction of the z-presentation of experimental data can be applied both for the analysis of stable particles and resonances as well. We consider that each type of an inclusive particle is characterized by a corresponding value of the parameter ϵ. The general scheme is the same but the properties of initial data should be taken into account. Among them are momentum, mass, quantum numbers, and particle identification. The method of identification is essential to separate possible mechanisms of the particle production [40,41]. We assume that, at the level of cross sections, mechanisms of soft and hard production of the same particle is described by the unique function $\psi(z)$. Both regions demonstrate the self-similarity but different scale dependence. Based on the obtained results one can expect that analogous would hold also for particles with heavier flavor content (c, s, t). Here suitable experimental data sets are needed to fix the parameters δ_1, δ_2, ϵ_a, ϵ_b, and c. On the other hand the assumption of the flavor independence of the function $\psi(z)$ can be used if data are known at least in the restricted (usually low-z) kinematical range. In such a case it is possible to exploit the asymptotic behavior of the scaling function for π^0 which is known up to $z = 30$. Using the data on (ϕ, ρ^0, $K^\star$, Λ, Ξ, J/ψ) production including π^0 cross sections one can perform the combined analysis [42,43] in z-presentation. Nevertheless direct verification of the universality of the scaling function for various types of particles both in the low-z and high-z-region is desirable.

Let us briefly discuss likeness and distinction which takes place for the phenomenological description of inclusive cross sections in terms of the scaling variables x_F, z and in the framework of pQCD. Primarily note that both variables are dimensionless and were found from the phenomenological analysis of experimental data. The behavior of cross sections $Ed^3\sigma/dp^3 \sim x_F^n(1 - x_F)^m$ for $x_F \to 0$ and $x_F \to 1$ are governed by Regge trajectories and the quark-counting rules [13,14]. The exponents n and m are found experimentally as energy, momentum, and angular dependent parameters. The scaling of spectra in x_F-presentation is fulfilled for $x_F \to 1$ only. It is violated in the central interaction region. Different modifications [44] of x_F were suggested to restore the x_F-scaling but they are of no consecutive physical reasoning. In the central

rapidity range, the variable $x_T = 2p_T/\sqrt{s}$ was used for parametrization of cross sections, $Ed^3\sigma/dp^3 \sim p_T^{-l} f(x_T)$, at high p_T. The exponent l is usually not an integer number, it depends on energy $\sqrt{s}$, and its relation to the quark-counting rules is not too obvious.

The procedure for construction of the variable z and the function $\psi(z)$ is aimed to reflect the principles of locality, self-similarity, and fractality. In contrast to other scaling variables, z represents a fractal measure, i.e. the scale-dependent quantity. It means that the measure diverges, $z(\Omega) \to \infty$, as the resolution increases, $\Omega^{-1} \to \infty$. The resolution should be understood with respect to all constituent subprocesses which can contribute to the production of an inclusive particle with a given momentum p. The parameters δ and ϵ determine the fractal character of z and have a meaning of fractal dimensions. They were found to be constant over a wide range of $\sqrt{s}$, p_T, and η. Both self-similarity and fractality (the scale independence of $\psi(z)$) were established over a wide z-range.

The z-scaling gives strong constraint on the asymptotic behavior of $\psi(z)$ and consequently on $Ed^3\sigma/dp^3$. This behavior was confronted with the numerical predictions in the framework of pQCD presented at high p_T in Sec. IV. Calculations based on the NLO QCD were compared with RHIC data on π^0 meson production measured in pp collisions at $\sqrt{s} = 200$ GeV and a good agreement was found to be [45]. At the same time the description of spectra for charged ($h^{\pm}$) [26] and especially for strange (K^0_S, Λ, Ξ) hadrons [40,41] are sensitive to the phenomenological fragmentation functions. We consider that suitable constraints on phenomenology of PDFs and FFs are needed to verify the perturbative QCD in hadron collisions with high accuracy and establish predictive power of the theory in the nonperturbative region. This is feasible, in particular, in the asymptotic regime where the behavior of the scaling function $\psi(z)$ can be used to impose restrictions on the poor known gluon distribution function.

In the pQCD analysis [38,39,46–50] the structure and fragmentation functions are taken from experiments on deep inelastic scattering and e^+e^- annihilation processes. A strong Q^2-dependence (the scale dependence) of the structure functions in the low-x (< 0.01) and high-x (> 0.6) range is observed experimentally. Therefore the results (cross sections) based on the Q^2-evolution of the structure functions are model dependent in the range of high p_T as well. This is true in respect to sensitivity of the transverse momentum spectra on the renormalization, factorization, and hadronizations scales. One of the methods of the QCD analysis of structure functions is the Jacobi polynomial expansion method [51]. In the method the moments of structure functions satisfy the renormalization equation [52]. The solution of the equation gives the Q^2-evolution of the moments $M_n(Q^2) = \int_0^1 x^{n-2} F(x, Q^2) dx$ of the structure function $F(x, Q^2)$ governed by the fractal dimensions γ_n calculated in the perturbative QCD. In the leading order the solution for the nonsinglet structure function is written in the form $M_n(Q^2) = M_n(Q_0^2)[\alpha_S(Q^2)/\alpha_S(Q_0^2)]^{\gamma^{0,n}_{NS}/2\beta_0}$. The ratio $d^n_{NS} = \gamma^{0,n}_{NS}/2\beta_0$ for $n_f = 3$ is equal to 0.395, 0.775, 1.000, 1.162, and 1.289 for $n = 2$, 4, 6, 8, and 10, respectively [52]. The dependence of the running coupling constant α_S on Q^2 is governed by the renormalization equation. We would like to note that there is substantial difference between the QCD fractal dimensions γ_n and the phenomenological dimensions δ and ϵ in the z-scaling approach. The first ones are due to nonlinear interaction of quantum gluon fields and as a result violation of the dimension counting rule takes place. The latter determine fractal character of the scaling variable z in terms of the underlying constituent subprocesses in the space of the momentum fractions x_1, x_2, y_a, and y_b. Yet, there exists a common parallel between QCD fractal dimensions and the phenomenological fractal dimensions in the z-scaling scheme. Both of them determine the characteristic power increase of the corresponding fractal measures at small distances and both of them concern hadron interactions at small scales. The unlimited increase of the moments $M_n(Q^2)$ with the resolution Q^2 (anomalous dimensions are negative for $n < 1$) is a typical fractal property. Similar concerns the fractal measure z in the region where x_1, x_2, y_a, $y_b \to 1$. So, in the first case the change of external momentum scale $p_i \to \lambda p_i$ for the connected Green's function leads to the shift of the renormalization point μ and consequently to the change of the coupling constant α_S. The Green's function is not invariant under such a transformation. Therefore its dimension is modified by the adding of an anomalous part (''anomalous fractal dimension'') coming from the scale dependence of the running coupling constant α_S. Note that the variable z reveals properties of a fractal measure as the resolution increases while the moments ($M_n(Q^2)$) of the structure functions demonstrate such property only for $n < 1$ (low-x range). It is possible that the discrepancy between z-scaling and NLO QCD predictions for high p_T (high-z) [see Figs. 14(b), 15(b), 16(b), 17(b), and 18(b)] in the TeV energy region is due to the absence of the fractal property for M_n with $n > 1$.

VI. CONCLUSIONS

The generalized z-scaling for the inclusive particle production in proton-proton collisions was suggested. The scaling variable z is a function of the multiplicity density $dN_{ch}/d\eta|_0$ of charged particles in the central region of collision. The variable z depends on the parameters c, δ, and ϵ, interpreted as a specific heat of the produced medium, a fractal dimension of the proton, and a fractal dimension of the fragmentation process, respectively. A connection between the scaling variable z and the entropy S of the interacting system was established.

We have analyzed experimental data on inclusive cross sections of hadrons ($h^{\pm}$, π^-, K^-, K^0_S, $\bar{p}$, and Λ) measured in proton-proton collisions at FNAL, ISR, and RHIC. The data cover a wide range of collision energy, transverse momenta, and angles of the produced particles. Spectra from minimum-biased events and events with various multiplicity selection criteria have been studied. The energy, angular, and multiplicity independence of the scaling function was established. It gives strong constrains on the values of the parameters c, δ, and ϵ. It was shown that the parameters are constant in the considered kinematical region. The scaling is consistent with the parameters $c = 0.25$ and $\delta = 0.5$ for all types of the considered inclusive hadrons. The value of ϵ increases with the mass of the produced hadron. The shape of the scaling function $\psi(z)$ was found to be the same for different types of produced hadrons over a wide range of z.

The variable z has the character of a fractal measure. Fractal properties of z are determined by the parameters δ and ϵ which are interpreted as fractal dimensions in the space of the momentum fractions. The scaling function $\psi(z)$ manifests two regimes of the particle production. The hard regime is characterized by the power-law $\psi(z) \sim z^{-\beta}$ for large z. The soft processes correspond to the behavior of $\psi(z)$ for small z. The value of the slope parameter of the scaling curve decreases with z in this region. Based on the results of the performed analysis we conclude that z-scaling in proton-proton collisions is a regularity which reflects the self-similarity, locality, and fractality of the hadron interaction at the constituent level. It concerns the structure of the colliding objects, interactions of their constituents, and fragmentation process. Self-similar features of particle production dictated by the z-scaling give strong restriction on the asymptotic behavior of the inclusive spectra in the high-p_T region. This behavior is not reproduced in the TeV energy range by the NLO QCD evolution of the cross sections with the phenomenological parton distribution and fragmentation functions used in the present calculations.

We consider that experimental verification of the NLO QCD calculations and z-scaling predictions are important for further tests of the QCD and more precise specification of the phenomenological ingredients which enter the pQCD calculations at small scales. The obtained results may be exploited to search for and study new physics phenomena in the particle production over a wide range of collision energies, production angles, transverse momenta, and large multiplicities in proton-proton and nucleus-nucleus interactions at RHIC and LHC.

ACKNOWLEDGMENTS

The investigations have been partially supported by the IRP AVOZ10480505, by the Grant Agency of the Czech Republic under Contract No. 202/07/0079 and by the special program of the Ministry of Science and Education of the Russian Federation, Grant No. RNP.2.1.1.5409. Authors are grateful to A. Sidorov for fruitful discussions on QCD properties of Mellin's moments of deep inelastic structure functions.

APPENDIX A

The scaling variable z has the character of a fractal measure. The boundaries of its range are 0 and ∞. They are accessible at any collision energy. The variable z consists of a finite part z_0 and of a divergent factor Ω^{-1}. For a given reaction (1), the finite part is proportional to the transverse kinetic energy of the constituent subprocess consumed on the production of the inclusive particle (m_1) and its counterpart (m_2). The factor Ω^{-1} describes a resolution at which the subprocess can be singled out of this reaction. The $\Omega(x_1, x_2, y_a, y_b)$ is a relative number of all parton configurations containing the incoming constituents which carry the fractions x_1 and x_2 of the momenta P_1 and P_2 and which fragment to the inclusive particle (m_1) and its counterpart (m_2) with the corresponding momentum fractions y_a and y_b. The parameters δ_1 and δ_2 have relation to the fractal structure of the colliding objects (hadrons or nuclei). They are interpreted as fractal dimensions in the space of the momentum fractions. The parameters ϵ_a and ϵ_b characterize the fractal behavior of the fragmentation process in the final state. A common property of fractal measures is their divergence with the increasing resolution

$$z(\Omega) \to \infty \quad \text{if } \Omega^{-1} \to \infty. \tag{A1}$$

For an infinite resolution the whole reaction (1) degenerates to a single subprocess (4), all momentum fractions become unity ($x_1 = x_2 = y_a = y_b = 1$) and $\Omega = 0$. This kinematical limit corresponds to the fractal limit $z = \infty$.

In the general case, the momentum fractions are determined from a principle of a minimal resolution of the fractal measure z. The principle states that the resolution Ω^{-1} should be minimal with respect to all binary subprocesses (4) in which the inclusive particle m_1 with the momentum p can be produced. This singles out the underlying interaction of the constituents which satisfies the condition (5). This condition can be conveniently written in the form

$$x_1 x_2 - x_1 \lambda_2 - x_2 \lambda_1 - \lambda_0 = 0. \tag{A2}$$

Here we have used the notations (9)–(12) in which λ_1, λ_2, and λ_0 are explicit functions of y_a and y_b. For given values of y_a and y_b, the momentum fractions x_1 and x_2 are found from a maximum of the functional

$$\Omega(x_1, x_2, y_a, y_b) + \beta(x_1 x_2 - x_1 \lambda_2 - x_2 \lambda_1 - \lambda_0) \tag{A3}$$

with a Lagrange multiplicator β. Taking the derivatives of the expression (A3) with respect to x_1 and x_2 one can obtain the equation

$$(1 - x_2)(x_1 - \lambda_1) = \alpha(1 - x_1)(x_2 - \lambda_2), \tag{A4}$$

where $\alpha = \delta_2/\delta_1$ is the ratio of the fractal dimensions of the colliding objects. The explicit solution of the system of two Eqs. (A2) and (A4) gives the formulae (7) and (13)–(16). So the problem of finding a maximum of $\Omega(x_1, x_2, y_a, y_b)$ satisfying the condition (5) is reduced to a task to search for an unconstrained maximum of the function (17) of two independent variables y_a and y_b. This is solved for every value of the momentum p numerically.

There exists a connection between the variable z and entropy. The scaling variable (19) is proportional to the ratio

$$z \sim \frac{s_\perp^{1/2}}{W} \tag{A5}$$

of the transverse kinetic energy $s_\perp^{1/2}$ and the maximal value of the quantity

$$W(x_1, x_2, y_a, y_b) = (dN_{ch}/d\eta|_0)^c \cdot \Omega(x_1, x_2, y_a, y_b) \tag{A6}$$

in the space of the momentum fractions. The average multiplicity density $dN_{ch}/d\eta|_0$ of charged particles produced in the central region of the reaction (1) depends on a state of the produced medium in the colliding system. The parameter c characterizes properties of this medium. The quantity W is proportional to all parton and hadron configurations of the colliding system which can contribute to the production of the inclusive particle with the momentum p.

According to statistical physics, entropy of a system is given by a number of all statistical states W of the system as follows

$$S = \ln W. \tag{A7}$$

In thermodynamics, entropy for an ideal gas is determined by the formula

$$S = c_V \ln T + R \ln V + \text{const}, \tag{A8}$$

where c_V is a heat capacity and R is a universal constant. The temperature T and the volume V characterize a state of the system. Using Eqs. (A6) and (A7), we can write

$$S = c \ln[dN_{ch}/d\eta|_0] + \ln[(1 - x_1)^{\delta_1}(1 - x_2)^{\delta_2}(1 - y_a)^{\epsilon_a} \times (1 - y_b)^{\epsilon_b}]. \tag{A9}$$

Exploiting the analogy between Eqs. (A8) and (A9), we interpret the parameter c as a ''heat capacity'' of the produced medium. The multiplicity density $dN_{ch}/d\eta|_0$ of particles in the central region characterizes a ''temperature'' of the colliding system [53]. Provided that the system is in a local equilibrium, there exists a simple relation $dN_{ch}/d\eta|_0 \sim T^3$ for high temperatures and small chemical potentials. The second term in Eq. (A9) depends on the volume in the space of the momentum fractions $\{x_1, x_2, y_a, y_b\}$. This analogy emphasizes once more the interpretation of the parameters δ_1, δ_2, ϵ_a, and ϵ_b as fractal dimensions. In accordance with common arguments, the entropy (A9) increases with the multiplicity density and decreases with the increasing resolution Ω^{-1}. In the considered analogy, the principle of a minimal resolution Ω^{-1} with respect to all subprocesses satisfying the condition (5) is equivalent to the principle of a maximal entropy S of the rest of the colliding system (A9).

Using the principle of a maximal entropy $S(x_1, x_2, y_a, y_b)$ under the condition (5) one fixes the values of the momentum fractions x_i and y_i and singles out the most effective subprocess which underly the inclusive reaction (1). Assuming such a partition of an interacting system into a single constituent binary collision and the rest of all other microscopic configurations which lead to the produced multiplicity, some general conclusions on dynamics of the system can be made. The performed analysis shows that the values of y_b are considerably smaller than the values of y_a. It is fulfilled for all types of particles and kinematics under consideration. This means that the momentum balance in the production of an inclusive particle from a subprocess is more likely compensated by the states with a higher multiplicity of particles with smaller momenta than by a single particle with a higher momentum moving in the opposite direction. Such an asymmetry diminishes near the kinematical limit, where both y_a and y_b tend to unity. Another interesting observation is that the momentum fractions y_a and y_b decrease with the increasing collision energy. This corresponds to the scenario in which more multiplicity is produced from a single constituent interaction at higher center-of-mass energies $s^{1/2}$. We stress that the general features mentioned above do not depend on the specific values of the fractal dimensions δ and ϵ.

Let us note that the entropy (A7) is determined up to an arbitrary constant $\ln W_0$. Dimensional units entering the definition of the entropy can be included within this constant. In particular, it allows to account for a relation between the dimensionless multiplicity density $dN_{ch}/d\eta|_0$ and the temperature. This degree of freedom is related to the transformation

$$z \to W_0 \cdot z, \qquad \psi \to W_0^{-1} \cdot \psi. \tag{A10}$$

In such a way the scaling variable and the scaling function are determined up to an arbitrary multiplicative constant. The constant W_0 is related to an absolute number of the microscopic states of the system. Its value is restricted by the positiveness of the entropy above some scale characterized by a maximal resolution Ω^{-1}. For the resolution corresponding to the fractal limit, W_0 is infinity. Thus, the transformation (A10) is connected with a renormalization of the fractal measure z in agreement with its physical interpretation (A5).

The procedure for the construction of the z-presentation of experimental data consists of several steps:

(1) First of all we take some experimental data sets on transverse momentum spectra of inclusive cross sections $Ed^3\sigma/dp^3$ corresponding to different collision energies $\sqrt{s}$, angles θ of the produced particles, and multiplicity classes N_{ch} of events. The charged particle multiplicity densities $dN_{ch}/d\eta|_0(s)$ in the central interaction region ($\eta = 0$) at these collision energies are required as well.
(2) The general formulae presented in Sec. II allow us to calculate the scalar invariants of all particle 4-momenta P_1, P_2, p and determine the fractions x_1, x_2, y_a, and y_b which correspond to the maximum of the functional (A3).
(3) The scaling variable z and the scaling function $\psi(z)$ are expressed via the momentum fractions, multiplicity densities $dN_{ch}/d\eta|_0(s)$, and the experimental data on the inclusive cross section $Ed^3\sigma/dp^3$.
(4) The assumption of self-similarity transforms to the requirement of the simultaneous description of all the data sets by a scaling function $\psi(z)$. This gives strong constraint on values of the parameters δ, ϵ, and c and allows us to determine them. The fractal dimensions δ and ϵ are sensitive to high-p_T parts of spectra as well as to spectra at small angles. The dependence on the type of the produced particle is regulated by the parameter ϵ. The value of c is determined from multiplicity dependence of the cross sections.

APPENDIX B

The invariant differential cross section for the production of the inclusive particle is normalized as follows

$$\int E\frac{d^3\sigma}{dp^3}dyd^2p_\perp = \sigma_{\rm inel}N. \tag{B1}$$

The $\sigma_{\rm inel}$ is the inelastic cross section and N is the average multiplicity. The differential cross section of identified hadrons of a certain type is normalized to the corresponding average multiplicity of this type. The inclusive cross section can be expressed in terms of κ_1 and κ_2,

$$E\frac{d^3\sigma}{dp^3} = -\frac{1}{2\pi}\frac{\sqrt{(P_1P_2)^2 - M_1^2M_2^2}}{[(P_1P_2) - M_1M_2]^2}\frac{d^2\sigma}{d\kappa_1 d\kappa_2}. \tag{B2}$$

In the region of high energies, the formula can be written in an approximate form

$$E\frac{d^3\sigma}{dp^3} = -\frac{1}{\pi s A_1 A_2}\frac{d^2\sigma}{d\kappa_1 d\kappa_2}. \tag{B3}$$

We suppose that the inclusive cross section is given by a solution (18) as a function of a single variable $z = z(\kappa_1, \kappa_2)$. Another independent combination of κ_1 and κ_2 is the NN center-of-mass rapidity

$$y = \frac{1}{2}\ln\frac{\kappa_1}{\kappa_2} + \frac{1}{2}\ln\frac{A_1}{A_2}. \tag{B4}$$

Using both sets of independent variables, we obtain

$$\int\frac{d^2\sigma}{d\kappa_1 d\kappa_2}d\kappa_1 d\kappa_2 = \int\frac{d^2\sigma}{dydz}dydz = \sigma_{\rm inel}\int\tilde{\rho}(y)\tilde{\psi}(z,y)dydz = \sigma_{\rm inel}N. \tag{B5}$$

A detailed analysis of the experimental data on the angular properties of the scaling function has shown that the factorization

$$\frac{d^2\sigma}{d\eta dz} = \sigma_{\rm inel}\rho(\eta)\psi(z) \tag{B6}$$

is valid when pseudorapidity η rather than rapidity y is used. Here $\rho(\eta) \equiv dN/d\eta$ is the pseudorapidity density of particles of the considered type. The quantity $dN/d\eta$ enters the formula (25) in the normalization of the scaling function $\psi(z)$. Exploiting the relation between the rapidity y and the NN center-of-mass pseudorapidity η,

$$p_T\sinh\eta = m_T\sinh y, \tag{B7}$$

one can express the pseudorapidity density of particles in the following form

$$\frac{dN}{d\eta} \equiv \frac{dN}{dy}(\eta)\frac{dy}{d\eta} = \frac{dN}{dy}(\eta)\frac{p_T\cosh\eta}{m_T\cosh y} = \frac{dN}{dy}(\eta)\frac{p}{E}. \tag{B8}$$

The rapidity densities $dN/dy(\eta)$ were obtained from the normalization constants of the p_T spectra measured at various angles θ. The parametrizations of the spectra are often expressed as functions of the transverse momentum p_T or the transverse mass $m_T = (p_T^2 + m_1^2)^{1/2}$. Hence we have fitted the corresponding transverse momentum distributions by different functions. In dependence on the spectral shapes, we have used a power-law function

$$E\frac{d^3\sigma}{dp^3} = \frac{\sigma_{\rm inel}}{\pi}\frac{dN}{dy}(\eta)\frac{2(n-1)(n-2)}{(n-3)^2\langle p_T\rangle^2}\left(1 + \frac{2p_T}{\langle p_T\rangle(n-3)}\right)^{-n}, \tag{B9}$$

Levi function

$$E\frac{d^3\sigma}{dp^3} = \frac{\sigma_{\rm inel}}{\pi}\frac{dN}{dy}(\eta)\frac{(n-1)(n-2)}{2nT[m_1(n-2)+nT]} \times\left(1 + \frac{m_T - m_1}{nT}\right)^{-n}, \tag{B10}$$

exponential function

$$E\frac{d^3\sigma}{dp^3} = \frac{\sigma_{\rm inel}}{\pi}\frac{dN}{dy}(\eta)\frac{1}{2T(m_1+T)}\exp\left[\frac{-(m_T - m_1)}{T}\right], \tag{B11}$$

or Boltzman function

$$E\frac{d^3\sigma}{dp^3} = \frac{\sigma_{\rm inel}}{\pi}\frac{dN}{dy}(\eta)\frac{m_T}{2T(m_1^2+2m_1T+2T^2)} \times \exp\left[\frac{-(m_T-m_1)}{T}\right]. \quad \text{(B12)}$$

For inclusive spectra dependent on multiplicities, the extracted values of $dN/dy(\eta)$ are functions of the multiplicity selection criteria characterized by different total charged multiplicity densities $dN_{ch}/d\eta|_0$.

The derivatives $\partial\eta/\partial\kappa_i$ which enter the Jacobian (26) can be expressed directly. Using Eq. (B4) and the expressions

$$\kappa_1 \simeq \frac{E+p\cos\theta}{A_1\sqrt{s}}, \qquad \kappa_2 \simeq \frac{E-p\cos\theta}{A_2\sqrt{s}}, \quad \text{(B13)}$$

we can rewrite the relation (B7) as follows

$$\sinh\eta = \frac{\sqrt{s}}{2}\frac{(A_1\kappa_1 - A_2\kappa_2)}{\sqrt{sA_1A_2\kappa_1\kappa_2 - m_1^2}}. \quad \text{(B14)}$$

From differentiating one can obtain

$$\frac{\partial\eta}{\partial\kappa_1} = +\frac{A_1\sqrt{s}}{2} \times \frac{sA_2\kappa_2(A_1\kappa_1+A_2\kappa_2)-2m_1^2}{(sA_1A_2\kappa_1\kappa_2-m_1^2)\sqrt{s(A_1\kappa_1+A_2\kappa_2)^2-4m_1^2}}, \quad \text{(B15)}$$

$$\frac{\partial\eta}{\partial\kappa_2} = -\frac{A_2\sqrt{s}}{2} \times \frac{sA_1\kappa_1(A_1\kappa_1+A_2\kappa_2)-2m_1^2}{(sA_1A_2\kappa_1\kappa_2-m_1^2)\sqrt{s(A_1\kappa_1+A_2\kappa_2)^2-4m_1^2}}. \quad \text{(B16)}$$

Inserting κ_1 and κ_2 from (B13), we get

$$\frac{\partial\eta}{\partial\kappa_1} = +\frac{A_1\sqrt{s}}{2p_T^2}(p - E\cos\theta), \quad \text{(B17)}$$

$$\frac{\partial\eta}{\partial\kappa_2} = -\frac{A_2\sqrt{s}}{2p_T^2}(p + E\cos\theta). \quad \text{(B18)}$$

The derivatives $\partial z/\partial\kappa_i$ in (26) were calculated numerically.

Let us make a brief comment on suitability of the utilization of pseudorapidity instead of rapidity in the factorization of the cross section. The main quantitative difference is in the Jacobian. In the case of rapidity one should use $\partial y/\partial\kappa_1 = +1/(2\kappa_1)$ and $\partial y/\partial\kappa_2 = -1/(2\kappa_2)$ instead of (B17) and (B18) with a replacement of $dN/d\eta$ by dN/dy in the formula (25). We have verified that, for pions, this would lead to perceivable discrepancy between z-presentation of data in the central and fragmentation region for small transverse momenta ($z \lesssim 1$). The difference is even more evident for heavier particles for which it starts to occur at larger values of z. When using the pseudorapidity instead of rapidity, the angular independence of the scaling function for all particles (pions, kaons, and antiprotons) is preserved up to very small momenta and production angles. In this sense z-presentation of data on inclusive cross sections is naturally connected with geometry in particle production.

Finally, we will examine the transverse kinetic energy $s_\perp^{1/2}$ (21) which enters definition of the scaling variable z. In the central interaction region, the formulae (22) and (23) can be expressed in a simple approximate form. We have checked therefore that $\lambda_1\lambda_2 \simeq \kappa_1\kappa_2/y_a^2$ is valid with good accuracy in this region. The transverse energy balance in the constituent subprocess is guarantied by the identity

$$\chi_1\chi_2 = \mu_1\mu_2 = \lambda_1\lambda_2 + \lambda_0. \quad \text{(B19)}$$

Using these relations and neglecting the masses $M_i\lambda_i$ and $M_i\chi_i$ of the interacting constituents, we get

$$T_a \simeq y_a\sqrt{\lambda_1\lambda_2 2P_1P_2} - m_1 \simeq \sqrt{\kappa_1\kappa_2 2P_1P_2} - m_1 \simeq \sqrt{p_\perp^2+m_1^2} - m_1 \quad \text{(B20)}$$

and

$$\begin{aligned} T_b &\simeq y_b\sqrt{\chi_1\chi_2 2P_1P_2} - m_2 \\ &= y_b\sqrt{(\lambda_1\lambda_2+\lambda_0)2P_1P_2} - m_2 \\ &\simeq y_b\sqrt{(p_\perp^2+m_1^2)/y_a^2 + m_2^2/y_b^2 - m_1^2/y_a^2} - m_2 \\ &= \sqrt{\tilde{p}_\perp^2+m_2^2} - m_2. \end{aligned} \quad \text{(B21)}$$

In the last equation we have used the transverse momentum balance

$$p_\perp/y_a = \tilde{p}_\perp/y_b, \quad \text{(B22)}$$

valid in the constituent subprocess. The symbols p and $\tilde{p}$ stand for the momenta of the inclusive particle (m_1) and its counterpart (m_2), respectively. The above approximations are valid with an accuracy better that 10% for all analyzed spectra in the central interaction region. They are however not applicable in the fragmentation region ($\theta \lesssim 10^0$) where the expressions on the right-hand side of the relations (B20) and (B21) significantly differ from the formulae (22) and (23). This difference is more pronounced in the case of kaons and antiprotons and other particles with heavier masses.

[1] E. Eichten, K. Lane, and M. Peskin, Phys. Rev. Lett. **50**, 811 (1983); E. Eichten, I. Hinchliffe, K. Lane, and C. Quigg, Rev. Mod. Phys. **56**, 579 (1984).

[2] I. Antoniadis, in Proceedings of European School of High-Energy Physics, Beatenberg, Switzerland, 2001, edited by N. Ellis and J. March-Russul (CERN, Geneva, 2000), p. 301.

[3] C. G. Lester, Czech. J. Phys. **54**, A303 (2004).

[4] L. Nottale, *Fractal Space-Time and Microphysics* (World Scientific, Singapore, 1993).B. Mandelbrot, *The Fractal Geometry of Nature* (Freeman, San Francisco, 1982).

[5] R. P. Feynman, Phys. Rev. Lett. **23**, 1415 (1969).

[6] J. D. Bjorken, Phys. Rev. **179**, 1547 (1969); J. D. Bjorken and E. A. Paschos, Phys. Rev. **185**, 1975 (1969).

[7] P. Bosted *et al.*, Phys. Rev. Lett. **49**, 1380 (1982).

[8] J. Benecke *et al.*, Phys. Rev. **188**, 2159 (1969).

[9] A. M. Baldin, Sov. J. Part. Nucl. **8**, 429 (1977).

[10] V. S. Stavinsky, Sov. J. Part. Nucl. **10**, 949 (1979).

[11] G. A. Leksin, Report No. ITEF-147, 1976; in *Proceedings of the XVIII International Conference on High Energy Physics, Tbilisi, USSR, 1976*, edited by N. N. Bogolubov (JINR, Dubna, 1977), p. A6-3.

[12] Z. Koba, H. B. Nielsen, and P. Olesen, Nucl. Phys. **B40**, 317 (1972).

[13] V. A. Matveev, R. M. Muradyan, and A. N. Tavkhelidze, Sov. J. Part. Nucl. **2**, 7 (1971); Lett. Nuovo Cimento Soc. Ital. Fis. **5**, 907 (1972); **7**, 719 (1973).

[14] S. Brodsky and G. Farrar, Phys. Rev. Lett. **31**, 1153 (1973); Phys. Rev. D **11**, 1309 (1975).

[15] A. Bialas and R. Peschanski, Nucl. Phys. **B273**, 703 (1986); **B308**, 857 (1988).

[16] I. M. Dremin, JETP Lett. **45**, 643 (1987).

[17] E. A. DeWolf, I. M. Dremin, and W. Kittel, Phys. Rep. **270**, 1 (1996).

[18] I. Zborovský, Yu. A. Panebratsev, M. V. Tokarev, and G. P. Škoro, Phys. Rev. D **54**, 5548 (1996); I. Zborovský, M. V. Tokarev, Yu. A. Panebratsev, and G. P. Škoro, Phys. Rev. C **59**, 2227 (1999); M. V. Tokarev and T. G. Dedovich, Int. J. Mod. Phys. A **15**, 3495 (2000); M. V. Tokarev, O. V. Rogachevski, and T. G. Dedovich, J. Phys. G **26**, 1671 (2000); JINR, Dubna, Report No. E2-2000-90, 2000; M. Tokarev, I. Zborovský, Yu. Panebratsev, and G. Skoro, Int. J. Mod. Phys. A **16**, 1281 (2001); M. Tokarev, arXiv:hep-ph/0111202; M. Tokarev and D. Toivonen, arXiv:hep-ph/0209069; G. P. Skoro, M. V. Tokarev, Yu. A. Panebratsev, and I. Zborovský, arXiv:hep-ph/0209071; M. V. Tokarev, G. L. Efimov, and D. E. Toivonen, Phys. At. Nucl. **67**, 564 (2004); M. Tokarev, Acta Phys. Slovaca **54**, 321 (2004); M. V. Tokarev and T. G. Dedovich, Phys. At. Nucl. **68**, 404 (2005).

[19] I. Zborovský and M. V. Tokarev, Phys. Part. Nucl. Lett. **3**, 312 (2006).

[20] D. Antreasyan *et al.*, Phys. Rev. D **19**, 764 (1979).

[21] B. Alper *et al.* (BS Collaboration), Nucl. Phys. **B100**, 237 (1975).

[22] F. W. Büsser *et al.* (CCRS Collaboration), Nucl. Phys. **B106**, 1 (1976).

[23] D. Drijard *et al.* (CDHW Collaboration), Nucl. Phys. **B208**, 1 (1982).

[24] D. E. Jaffe *et al.*, Phys. Rev. D **40**, 2777 (1989).

[25] J. Adams *et al.* (STAR Collaboration), Phys. Rev. Lett. **91**, 172302 (2003).

[26] J. Adams *et al.* (STAR Collaboration), Phys. Lett. B **637**, 161 (2006).

[27] J. Adams *et al.* (STAR Collaboration), Phys. Lett. B **616**, 8 (2005).

[28] J. Adams and M. Heinz (STAR Collaboration), arXiv:nucl-ex/0403020.

[29] D. R. Ward, Report No. CERN-EP/87-178, 1978 (unpublished); W. Thomé *et al.*, Nucl. Phys. **B129**, 365 (1977).

[30] M. G. Albrow *et al.* (CHLM Collaboration), Nucl. Phys. **B56**, 333 (1973).

[31] I. Arsene *et al.* (BRAHMS Collaboration), Phys. Rev. Lett. **93**, 242303 (2004).

[32] J. E. Gans, Ph.D. thesis, Yale University, 2004.

[33] R. Witt (STAR Collaboration), J. Phys. G **31**, S863 (2005).

[34] M. V. Tokarev, in Proceedings of the International Workshop on "Relativistic Nuclear Physics: from Hundreds of MeV to TeV," Varna, Bulgaria, 2001 (JINR, Dubna, 2001), Vol. 1, p. 280.

[35] F. Aversa, P. Chiappetta, M. Greco, and J. Ph. Guillet, Phys. Lett. B **210**, 225 (1988); **211**, 465 (1988); Nucl. Phys. **B327**, 105 (1989).

[36] H. L. Lai *et al.*, Phys. Rev. D **55**, 1280 (1997); Eur. Phys. J. C **12**, 375 (2000); arXiv:hep-ph/9903282; J. Pumplin *et al.*, J. High Energy Phys. 07 (2002) 012; arXiv:hep-ph/0201195.

[37] A. D. Martin, R. G. Roberts, W. J. Stirling, and R. S. Thorne, Eur. Phys. J. C **14**, 133 (2000).

[38] B. A. Kniehl, G. Kramer, and B. Potter, Nucl. Phys. **B582**, 514 (2000).

[39] J. Binnewies, B. A. Kniehl, and G. Kramer, Z. Phys. C **65**, 471 (1995); Phys. Rev. D **52**, 4947 (1995).

[40] B. I. Abelev *et al.*, arXiv:nucl-ex/0607033; M. Heinz, in Proceedings of the 22nd Winter Workshop on Nuclear Dynamics, La Jolla, CA, 2006 (unpublished); http://rhic.physics.wayne.edu/ bellwied/sandiego06/.

[41] J. Adams *et al.*, Phys. Rev. C **71**, 064902 (2005); arXiv:nucl-ex/0412019.

[42] M. V. Tokarev and I. Zborovský, in Proceedings of the XVIII Inernational Baldin Seminar on High Energy Physics Problems "Relativistic Nuclear Physics and Quantum Chromodynamics," Dubna, Russia, 2006 (unpublished).

[43] M. V. Tokarev, JINR, Dubna, Report No. E2-2004-178, 2006; in Proceedings of 8th International Workshop "Relativistic Nuclear Physics: From hundreds of MeV to TeV," Dubna, Russia, 2005, (JINR, Dubna, 2006), p. 278; arXiv:hep-ph/0405230.

[44] J. R. Johnson *et al.*, Phys. Rev. D **17**, 1292 (1978); A. Brenner *et al.*, Phys. Rev. D **26**, 1497 (1982).

[45] S. S. Adler *et al.* (PHENIX Collaboration), Phys. Rev. Lett. **91**, 241803 (2003); H. Buesching (PHENIX Collaboration), in Proceedings of the International Workshop Hot Quark 06, Villasimius, Sardinia, Italy, 2006 (unpublished); http://hq2006.bnl.gov; F. Simon (STAR Collaboration), in Proceedings of the 17th International Spin Physics Symposium, SPIN2006, Kyoto, Japan, 2006 (unpublished); http://www-nh.scphys.kyoto-u.ac.jp/SPIN2006/.

[46] L. Bourhis, M. Fontannaz, J. Ph. Guillet, and M. Werlen, Eur. Phys. J. C **19**, 89 (2001); arXiv:hep-ph/0009101.

[47] S. Kretzer, Phys. Rev. D **62**, 054001 (2000); arXiv:hep-ph/0003177.
[48] P. Aurenche *et al.*, Eur. Phys. J. C **13**, 347 (2000).
[49] P. Aurenche, R. Baier, M. Fontannaz, and D. Schiff, Nucl. Phys. **B297**, 661 (1988); P. Aurenche *et al.*, Phys. Rev. D **73**, 094007 (2006).
[50] S. Alekhin, Phys. Rev. D **68**, 014002 (2003); JETP Lett. **82**, 628 (2005); arXiv:hep-ph/0508248; S. Alekhin, K. Melnikov, and F. Petriello, Phys. Rev. D **74**, 054033; Phys. Rev. D **74**, 054033 (2006).
[51] G. Parisi and N. Sourlas, Nucl. Phys. **B151**, 421 (1979); V. G. Krivokhizhin *et al.*, Z. Phys. C **36**, 51 (1987); **48**, 347 (1990); A. L. Kataev, G. Parente, A. V. Sidorov, Phys. Part. Nucl. **34**, 20 (2003).
[52] A. J. Buras, Rev. Mod. Phys. **52**, 199 (1980).
[53] J. Cleymans and K. Redlich, Phys. Rev. C **60**, 054908 (1999).